



ERA-40 Project Report Series

10. Reanalysis and Reforecast of Three Major European Storms of the 20th Century Using the ECMWF Forecasting System

Thomas Jung, Ernst Klinker and Sakari Uppala

European Centre for Medium-Range Weather Forecasts
Europäisches Zentrum für mittelfristige Wettervorhersage
Centre européen pour les prévisions météorologiques à moyen terme

Series: ECMWF ERA-40 Project Report Series

A full list of ECMWF Publications can be found on our web site under:

<http://www.ecmwf.int/publications/>

Contact: library@ecmwf.int

©Copyright 2003

European Centre for Medium Range Weather Forecasts
Shinfield Park, Reading, RG2 9AX, England

Literary and scientific copyrights belong to ECMWF and are reserved in all countries. This publication is not to be reprinted or translated in whole or in part without the written permission of the Director. Appropriate non-commercial use will normally be granted under the condition that reference is made to ECMWF.

The information within this publication is given in good faith and considered to be true, but ECMWF accepts no liability for error, omission and for loss or damage arising from its use.

Reanalysis and Reforecast of Three Major
European Storms of the 20th Century Using the
ECMWF Forecasting System

Thomas Jung, Ernst Klinker and Sakari Uppala

Research Department

November 2003

Submitted to Meteor. Appl.

Abstract

The latest ECMWF forecasting system is used together with historical observational data to reanalyse three major European storms of the 20th century and to assess their predictability. The storms considered are the Dutch storm of 1 February 1953, the Hamburg storm of 17 February 1962, and the British/French October storm of 1987. Common to all these storms is their severity that caused large loss of life and widespread damage.

Reanalysis of the storms is based on 3D-Var and 4D-Var assimilation schemes at different horizontal resolutions (T159 and T511). Further, the deterministic forecast skill of the storms is studied. The deterministic forecasts are supplemented by probabilistic forecasts using the ECMWF Ensemble Prediction System (EPS).

It is shown that the basic characteristics of the Dutch and Hamburg storm are well predicted by the single deterministic forecasts 48 and 84 hours, respectively, in advance. Moreover, the large number of ensemble members showing realistic storms suggest rather little sensitivity of these storms to analysis uncertainties at this forecast range. From these results it is argued that reliable warnings for the Dutch and Hamburg storm could have been issued 48 and 84 hours, respectively, in advance, using the current ECMWF forecasting system.

Our capability to issue warnings for the October storm is more difficult to assess. Both deterministic and probabilistic forecasts indicate a major storm occurring in the area of interest up to 96 hours in advance with a timing error of about 12 hours. On the other hand, as with the then operational forecasts, the severity of the storm is still significantly underestimated by very short-range forecasts (12–24 hours) with the latest ECMWF forecasting system.

From the results presented in this study it is concluded—though keeping in mind the limited number of cases considered—that with the current forecasting system reliable predictions of European wind storms might be possible well into the near medium-range. This is particularly true given that nowadays more observations are available (especially satellite data). Furthermore, it is argued that Ensemble Prediction Systems are an important component of every early warning system for they allow an *a priori* quantification of the probability of the occurrence of severe weather events.

1 Introduction

One of the major challenges of meteorology in general and weather forecasting in particular is the successful prediction of severe weather events well in advance. This is because human lives and property are particularly vulnerable to such extreme events.

Weather forecasting has a long history. Its first appearance can be traced back as far as Ptolemy (ca. 160 A.D.) who introduced astro-meteorological practices which were widely used well into the 19th century (e.g. [Nebeker, 1995](#), p. 36). A major change took place during the 19th century with the invention of the synoptic method; synoptic maps were drawn on a daily basis and forecasters used these maps to subjectively forecast tomorrow's weather. The synoptic method was in use well into the mid-20th century¹. The foundation of modern weather forecasting was laid by V. Bjerknes in 1903 and L. F. Richardson in 1922 ([Richardson, 1922](#)) in the sense that they promoted the use of physics to predict weather. It was the development of computers in the 1940s and 1950s together the development of a set of filtered equations of motions, the quasi-geostrophic equations ([Charney, 1947](#)), which allowed von Neumann and members of his group to perform the first numerical weather forecasts. Around the mid-1950s numerical weather forecasting became operational in Sweden as well as in the United States and in the 1960s most of the other major operational weather centers followed. In the 1960s useful forecast skill did not last beyond 1–2 days, though.

¹Forecasts for Operation Overlord in June 1944 (Allies' invasion of Normandy), for example, were still based on the synoptic method (e.g. [Nebeker, 1995](#), for a detailed description).

Forecast skill has improved dramatically in recent decades. These improvements were due to different factors: the use of a set of more complete equations (primitive equations), increased horizontal and vertical representation, improved numerical schemes, the development of parameterizations of physical processes, the availability of new observational data (e.g., satellites), and improved techniques to determine the models' initial conditions (e.g., variational data assimilation). It is due to these developments that nowadays skilful forecasts can be performed ten days ahead (Simmons and Hollingsworth, 2001).

By the end of the 1980s weather forecasters were primarily guided by single forecasts—so-called best-guess deterministic forecasts. The availability of only one single deterministic forecast has some inherent difficulties, though. This is because forecasts generally are sensitive to small initial perturbations (Lorenz, 1963; Rabier et al., 1996) and this sensitivity is flow-dependent (e.g., Palmer, 1988; Ferranti et al., 2002); that is, for some flows the initial growth of analysis errors is large whereas for others analysis errors may grow much slower or even conceivably decay. This flow-dependence of error growth, which is a consequence of the nonlinearity of the governing equations (e.g., Palmer, 1993), suggests that some flows are potentially more predictable than others and it would be helpful for weather forecasters to know in advance whether the atmosphere is in a potentially predictable or rather unpredictable state in order to issue reliable early warnings.

Given that single deterministic forecasts do not give any direct information about the sensitivity of the forecast to initial perturbations, by the end of the 1980s forecasters had to rely on their experience, the comparison of deterministic forecasts from different centres, and the inconsistency of forecasts started at different initial dates (poor man's ensembles) in order to assess the reliability of forecasts. A more systematic approach to *a priori* assess the forecast skill became operational in the early 1990s at several weather forecasting centers (Palmer et al., 1993; Toth and Kalnay, 1993; Molteni et al., 1996; Houtekamer et al., 1996). This technique, which is *probabilistic* rather than *deterministic*, is known as ensemble forecasting. Rather than performing only one integration, an ensemble of forecasts is performed starting from slightly perturbed initial conditions, with a perturbation size that is consistent with analysis uncertainties. A large spread of the ensemble indicates little predictability (in an average sense), whereas low spread suggests that predictability of the flow is rather high. It is worth noting that the ensemble approach is particularly valuable in the context of the present study, that is, for severe weather prediction. This is because low pressure systems tend to rapidly intensify in regions of large instabilities; and it is in these regions that the growth of initial errors tends likewise to be most extreme (Buizza and Palmer, 1995).

The possibility to carry out case studies of historic weather events at ECMWF has been created by the ECMWF reanalysis project, ERA-40, where a modern analysis technique was applied to data for the period 1957-2002 (e.g. Uppala, 2002). The necessary observations and forcing fields were collected and produced for the period as an international collaboration. Preliminary results show that the quality of the medium range forecasts during 1957-2002 increases in time with the improving global observing system. Case studies as represented by this study complement the long-term reanalysis products since the full potential of the observations and the forecasting system can be better exploited during such short periods as considered here.

In this study the state-of-the-art ECMWF Integrated Forecasting System (IFS) is used to reanalyse and reforecast three major storms of the 20th century, namely the Dutch² storm of 1 February 1953, the Hamburg storm of 17 February 1962, and the storm that hit south England and north-west France during the night from 15 to 16 October 1987. A special observational dataset was obtained for the Dutch storm from NCEP. All three storms have in common that they were extremely intense leading to loss of lives and large damages. In a survey on historic storms of north-west Europe during the last 500 years, Lamb (1991) ranked all recorded extreme storms according to their severity. The Great Storm is number eight on this list, the Dutch storm number twelve, and the Hamburg storm number twenty-eight! However, the observing system during the storms is very different.

²Although we use the expression Dutch storm in this study it should be kept in mind that the storm also killed hundreds of people in the UK.

The Dutch storm happened before the IGY (International Geophysical Year 1958), the Hamburg storm belongs to the pre-satellite era and the October storm belongs to a full satellite period.

The aim of this study is to quantify the deterministic predictability of these storms using historic data along with the most recent cycles of the ECMWF Integrated Forecasting System. Furthermore, the ECMWF EPS is used to quantify the risk of severe weather and investigate how long in advance it would have been possible to issue reliable warnings to the public. Such an undertaking is not only of academic interest. It also allows to test the influence of recent changes of the forecasting system in the context of severe weather forecasting. Furthermore, it is hoped that a detailed joint study of major storms, using both, the deterministic and probabilistic approach, may help weather forecasters to gain further experience in the usage of ensemble forecasts for severe weather predictions.

The structure of the paper is as follows. In Section 2 a brief overview of those components of the ECMWF Integrated Forecasting System is given which are widely used throughout this study. In Section 3, 4 and 5 the Dutch storm, the Hamburg storm, and the Great October storm, respectively, are discussed. Each of these sections starts with a brief description of the evolution of the storm based on reanalyzed data. Where possible, reanalyzed features are compared with measurements published in historic chronicles. Then, the performance of deterministic forecasts in the short-range and medium-range are discussed. This is followed by a description of probabilistic forecasts based on the EPS. Finally, the results are discussed in Section 6.

2 Methods

The main tool used in this study is the ECMWF IFS. It comprises, among others, an atmospheric general circulation model, data assimilation schemes, and the EPS.

In this study two different cycles of the ECMWF forecasting system are used. The older cycle (23r4) was operational from 12 June 2001 to 21 January 2002. This cycle was the basis of the data assimilation system used for the production of the ECMWF 40-year reanalysis (ERA-40). ERA-40 assimilation was carried out using a resolution of T159 in horizontal and 60 levels in vertical (T159L60). This cycle is also used in this study to produce ERA-40-type reanalyses and reforecasts. If not stated otherwise ERA-40-type experiments are performed using the ERA-40 (T159L60) resolution. As in ERA-40 a 3D-Var data assimilation scheme (Courtier et al., 1998) is used in all ERA-40-type experiments.

Furthermore, experimentation is based on the model cycle (25r4), which was operational at ECMWF from 14 January to 6 October 2003. This cycle comprises changes to almost all components of the IFS (e.g., assimilation techniques, numerical methods, physical parameterizations, and data usage). An overview over the changes and their impacts on forecast quality is given elsewhere (Andersson et al., 2003). If not stated otherwise, all high-resolution (T511 and 60 vertical levels) deterministic forecasts are based on cycle 25r4. The analyses produced with cycle 25r4 are based on a revised version of the original 4D-Var data assimilation scheme introduced in 1997 (Rabier et al., 2000; Mahfouf and Rabier, 2000). The resolution for the outer loop of the data assimilation is T511. The inner loop computations are based on two resolutions, a preliminary analysis based on T95 and an improved subsequent estimate based on T159 computations. A data window of 12 hours is used throughout this study in the 4D-Var assimilations.

Moreover, the ECMWF EPS (Molteni et al., 1996) is widely used throughout this study. All ensemble forecasts are based on model cycle 25r4 using a horizontal resolution of T255 and 40 levels in the vertical (T255L40). This resolution is the same as that used for operational ensemble forecasts at ECMWF. Perturbations for the initial conditions are based on the singular vector technique using a T42L40 model based on simplified physics and an optimizations time of 48 hours. The target area is the Northern Hemisphere. The initial conditions are

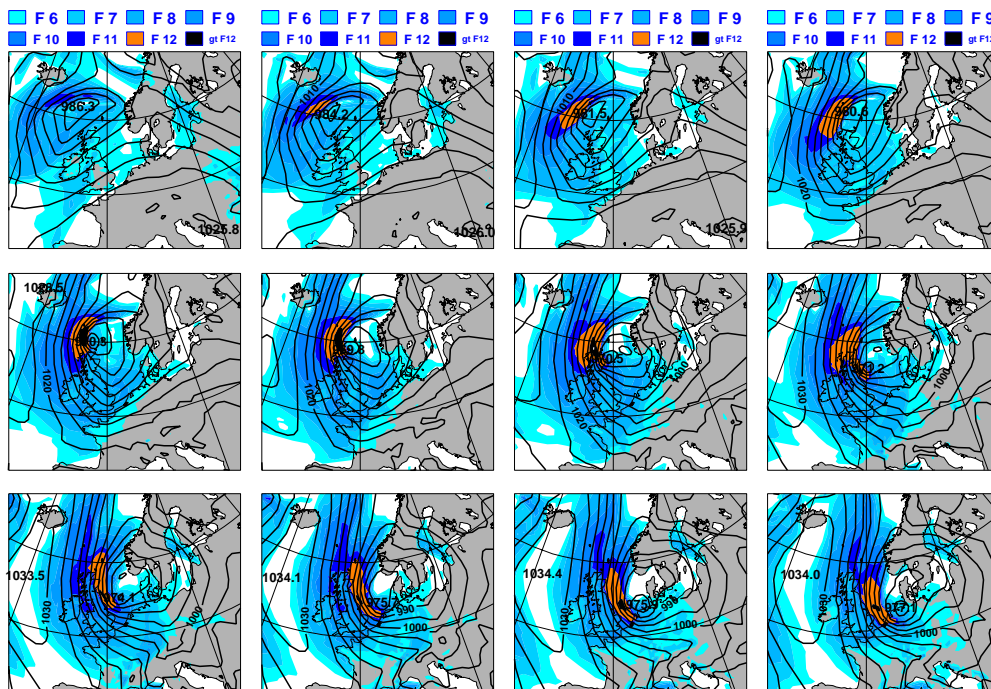


Figure 1: Mean sea level pressure (contours in hPa) and maximum wind gustiness (shading in Bft) for intervals of 3 hours from 15 UTC 30 January 1953 (upper left panel) to 00 UTC 1 February 1953 (lower right panel). The upper row is based on 3, 6, 9, and 12 hour forecasts with the high-resolution model (cycle 25r4) started at 12 UTC 30 January 1953. The middle and lower rows are based on corresponding forecast but started at 00 UTC 31 January and 12 UTC 31 January 1953, respectively. Officially, the Beaufort scale does not have values greater than 12 Bft. Here maximum gustiness greater than 12 Bft (black shading) is used for values exceeding 40 m/s.

further perturbed using evolved perturbations from two days earlier (Barkmeijer et al., 1999). Model errors are taken into account using stochastic physics (Buizza et al., 1999; Palmer, 2000). The ensemble comprises a total of 51 forecasts: one control forecast (T255L40) started from the operational analysis and 50 perturbed forecasts (T255L40) started from perturbed initial conditions as described above.

The magnitude of the initial perturbations used in the EPS should be consistent with analysis uncertainties. To estimate the magnitude of analysis uncertainties for the years under study (i.e., 1953, 1962, and 1987), short-range forecasts (24 hours) with the same model cycle (23r4) were used. These integrations were carried out in the context of the ERA-40 project. From these diagnostics it was found that the analysis uncertainties for the years 1953, 1962, and 1987 amount to about 1.5, 1.3, and 1.0 times the analysis uncertainty of the year 2003. For the EPS experiments described in this study the size of the initial perturbations has been adjusted correspondingly. However, for the three storms considered here, it has been found that the conclusions are not very sensitive to the actual magnitude of the initial perturbations.

3 The Dutch storm of 1 February 1953

The first storm considered is the Dutch storm whose gale force winds hit east England and the coast of the Netherlands during the night from 31 January to 1 February 1953. Onshore winds at the south-west coast of the Netherlands, which averaged 50–60 knots during a period of 6–9 hours prior to the time of high tide, let the sea level rise to heights that probably has not occurred during the past 400–500 years (van Ufford, 1953).

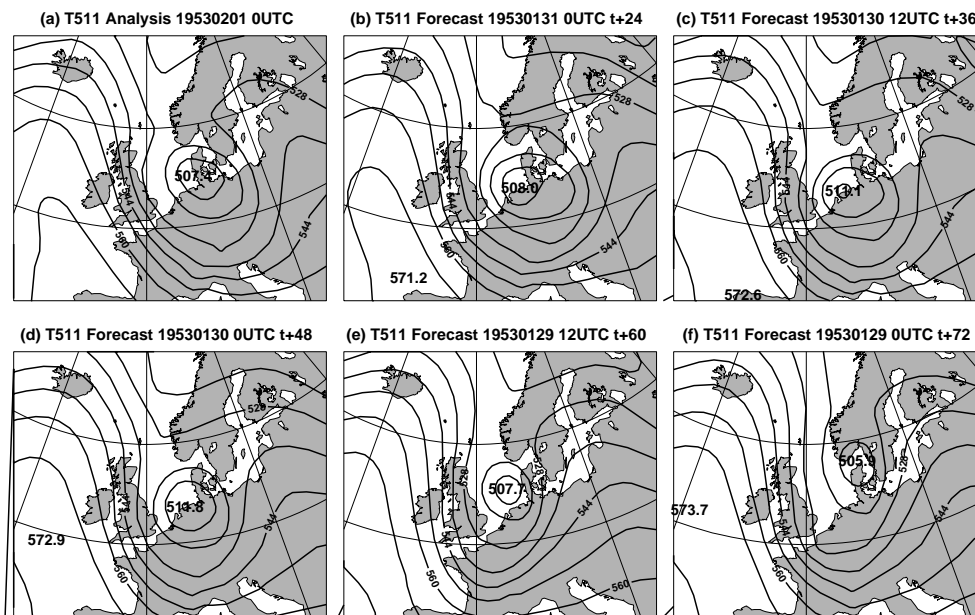


Figure 2: (a) Verifying 500 hPa geopotential height analysis (dm) along with corresponding short-range forecasts for 00 UTC 1 February 1953: (b) 24 hour, (c) 36 hour, (d) 48 hour, (e) 60 hour, and (f) 72 hour forecasts. Forecasts and analyses are based on the high-resolution model (25r4).

Most of the nearly 1800 casualties and damages—more than a thousand farms were destroyed—were a direct consequence of 50 dykes bursting almost simultaneously (van Ufford, 1953).

3.1 Evolution of the storm

The evolution of the cyclone and the associated wind field is shown in terms of mean sea level pressure and maximum wind gusts at 10 metres (Fig. 1). The gustiness is diagnosed on the basis of the parameterization of sub-grid scale turbulent momentum fluxes. It takes into account the horizontal wind speed at 10 metre along with the effect of surface friction and stability. This quantity has become a standard model post-processing parameter at ECMWF and is obtained from forecasts.

Rapid cyclogenesis occurred within 24 hours while the centre of the low pressure system moved from a position south-east of Iceland into northern Germany. In parallel, high pressure developed east of Great Britain which together with low pressure over Northern Europe led to the extreme pressure gradient over western parts of the North Sea (see also Hay and Laing, 1954; Lamb, 1991). The storm field with gusts of more than 33 m/s (12 Bft, red shading) approached Scotland from the north-west and moved into the North Sea along the east coast of Britain later. The analysed values are in good agreement with direct anemometer measurements from Orkney (mean winds of 45 m/s and gusts up to 55 m/s) (Hay and Laing, 1954). At times the reanalysed maximum gusts exceeded 40 m/s (black shading), in particular when the extreme pressure gradient reached south-western parts of the North Sea hitting the coast of the Netherlands. It was then that the maximum damage to the sea defences occurred.

Two particularities of the Dutch storm are worth mentioning. First, the actual storm surge was associated with a relatively large-scale intensive low-pressure system, for which one can expect relatively good predictability. Second, relatively strong winds in excess of 6 Bft (Beaufort scale 6) prevailed for a relatively long period (starting on 30 January 1953). It was this prevalence of strong winds that contributed to a piling up the water at

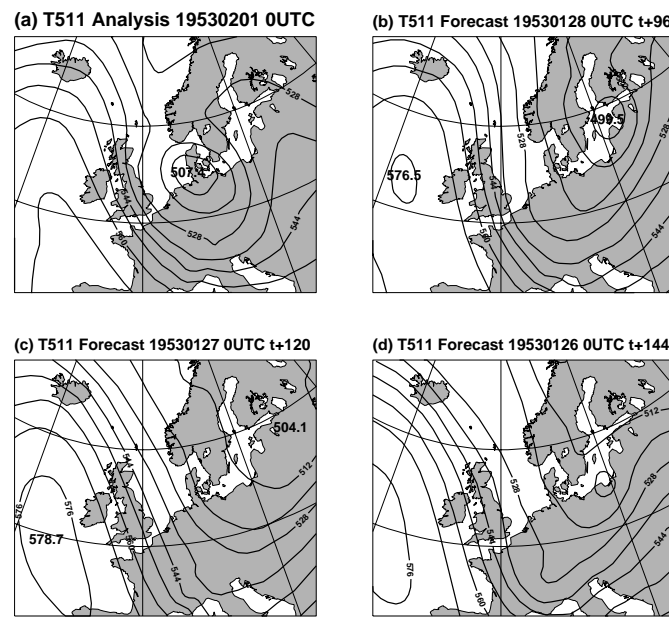


Figure 3: As in Fig. 2, except for medium-range forecasts: (b) D+4, (c) D+5, (d) D+6.

the coast of the Netherlands leading to the catastrophic events that took place in the early hours of 1 February 1953.

3.2 Deterministic Forecasts

Despite the fact that only conventional observations were available in 1953, the high-resolution analysis (T511) has been able to clearly identify the deep upper level low and the sharp pressure gradient east of the Atlantic ridge in the 500 hPa geopotential height field (Z_{500} , hereafter) associated with the Dutch storm (Fig. 2). It is interesting that the maximum gradient is found over mainland Britain and the Channel in a position noticeably to the west of the maximum surface winds as shown in Fig. 1 (bottom right panel).

The accuracy of the analysis is further underlined by the quality of the short-range forecast (24 and 48 hours). Both, at D+1 and D+2, the maximum gradient is close to the analysed one. For the D+3 forecast the centre of the cyclone is too far to the north-east, whereas the area of maximum gradient is still in the right position.

For the medium-range up to D+6, the model still predicts a north-westerly flow that is close to the analysed position (Fig. 3). However, the intensity of the forecast gradient is underestimated beyond D+4 and the predicted 500 hPa deep low is merely a trough of moderate intensity.

The analysed deep surface low has a central pressure of 976.3 hPa, which is only slightly higher than historical surface maps show. The position corresponds to the location of the mid-tropospheric low, thus showing little tilt in the vertical. However, the largest surface pressure gradient is found to the east of the upper level gradient. This surface gradient is associated with maximum surface winds along the east coast of Britain and the coast of the Netherlands as seen in Fig. 1 (lower right panel).

The remarkable model performance to reproduce a realistic mid-tropospheric flow is matched by the simulated evolution of the mean sea level pressure (MSLP) field (Fig. 4). Up to D+2 the forecasting system is able to produce an intensive cyclone centred in the German Bight. It is worth noting that the maximum gradient is slightly shifted to the west in the D+1 and D+2 forecast with the effect of an underestimation of the gradient in

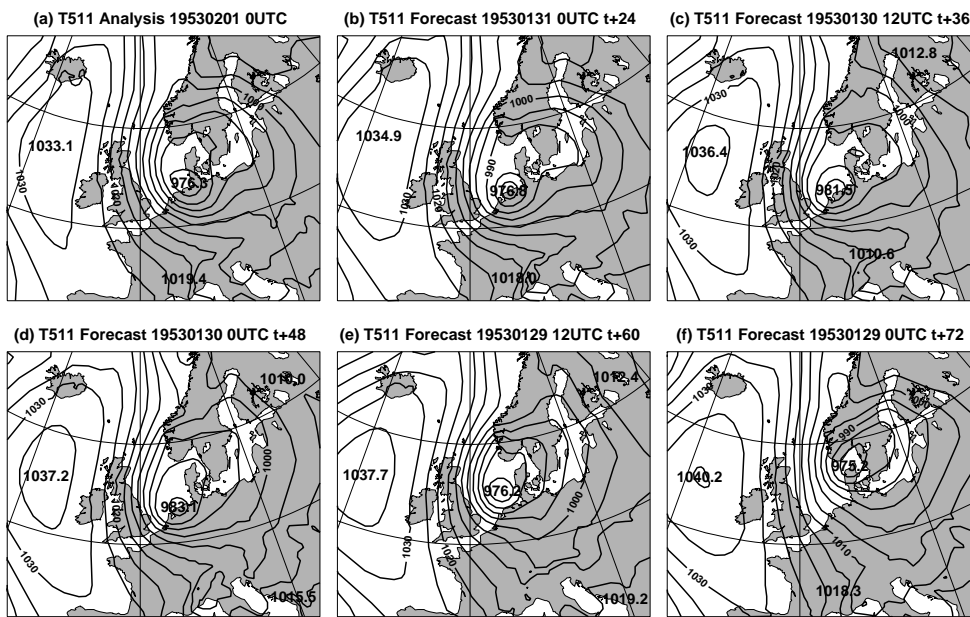


Figure 4: As in Fig. 2, except for mean sea level pressure (hPa).

north-easternmost parts of the Dutch coast. In the D+3 forecast the centre of the cyclone is predicted to be over Denmark and the area of the maximum gradient is located too far to the north.

In the medium-range (Fig. 5) the overall synoptic pattern of a north-westerly flow is captured; the signature for a major storm is lost, however. In particular the centre of the low pressure system is too far to the east. The Atlantic high pressure system is much better forecast in its longitudinal position, in particular in the D+4 and D+5 forecast.

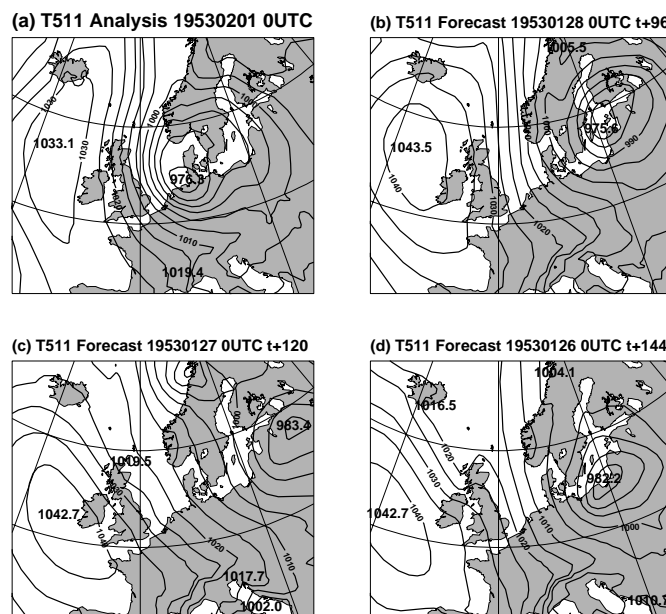


Figure 5: As in Fig. 3, except for mean sea level pressure (hPa).

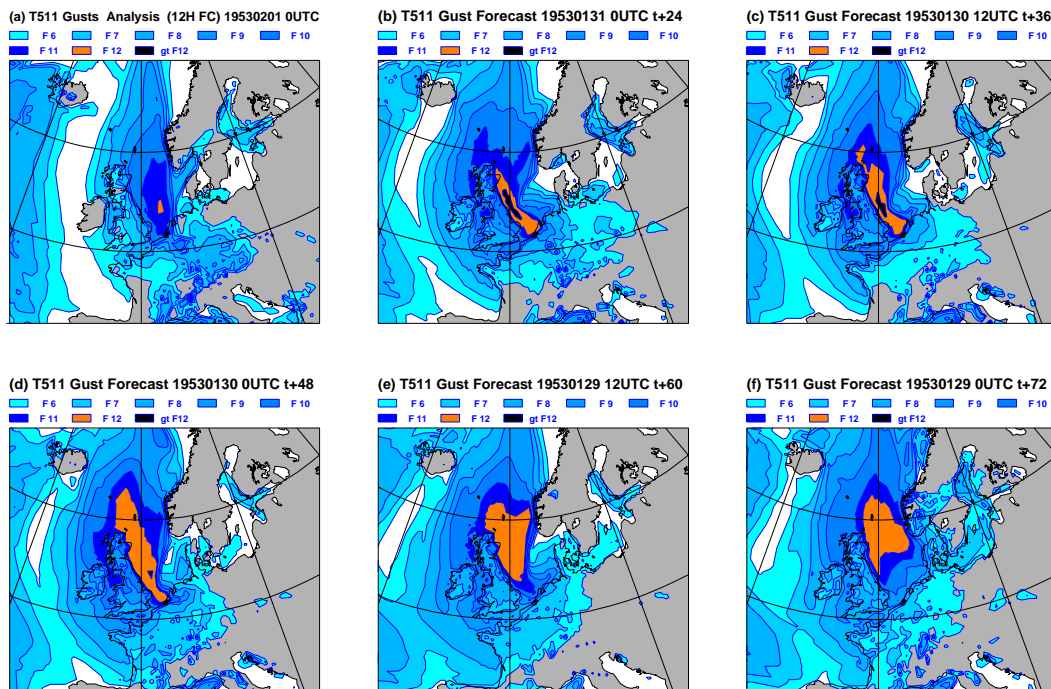


Figure 6: Maximum gusts (in Bft) for the (a) “analysis” (12-hour forecast) and (b) 24, (c) 36, (d) 48, (e) 60, and (f) 70 hour forecasts verifying at 00 UTC 1 February 1953. The gustiness represents maximum gusts over the last (b) 6 and (c)–(f) 12 hours of the respective forecast. Shading is done in terms of the Beaufort scale (from 6 to 12 Bft).

For the sea state and possible damage of sea defences and structural damages over land areas the gustiness is an important measure. Gusts of more than 33 m/s (12 Bft) are found over a long distance along the east coast of Britain in the analysis³ (Fig. 6). In the D+1 forecast the gusts are slightly stronger but they are distributed over a band that is clearly narrower than in the analysis. This is consistent with the fact that the surface pressure gradient is too far to the west in the short-range forecast. With increasing forecast length the gusts are weakened. At 36 and 48 hours, however, the signature of severe weather in the south-western North Sea is still there. At 60 hours an underestimation of the gustiness in south-western parts of the North Sea is evident. An extensive band of gusts exceeding 12 Bft, though, still exists over most parts of the northern half of the North Sea. At 72 hours a further weakening of the storm in south-western parts of the North Sea is evident. This forecast, therefore, suggests that there is little danger of a major storm surge to happened along the coast of the Netherlands.

The performance of the combined system of the atmospheric and wave model to produce exceptional wave heights is quite remarkable. More than 10-meter wave heights are found in the analysis in good agreement with recordings by the steamships *Tasso* and *Tinto* (see [Hay and Laing, 1954](#)). Similar values are found in the short-range at 36 and 48 hours (Fig. 7). At 24 hours wave heights are noticeably underestimated. This underestimation is consistent with the shift of the maximum surface pressure gradient to the west, which may have been sufficient to reduce the fetch necessary for producing large wave heights close to the coast of east Britain.

³The “analysis” is actually based on a 12 hour forecast.

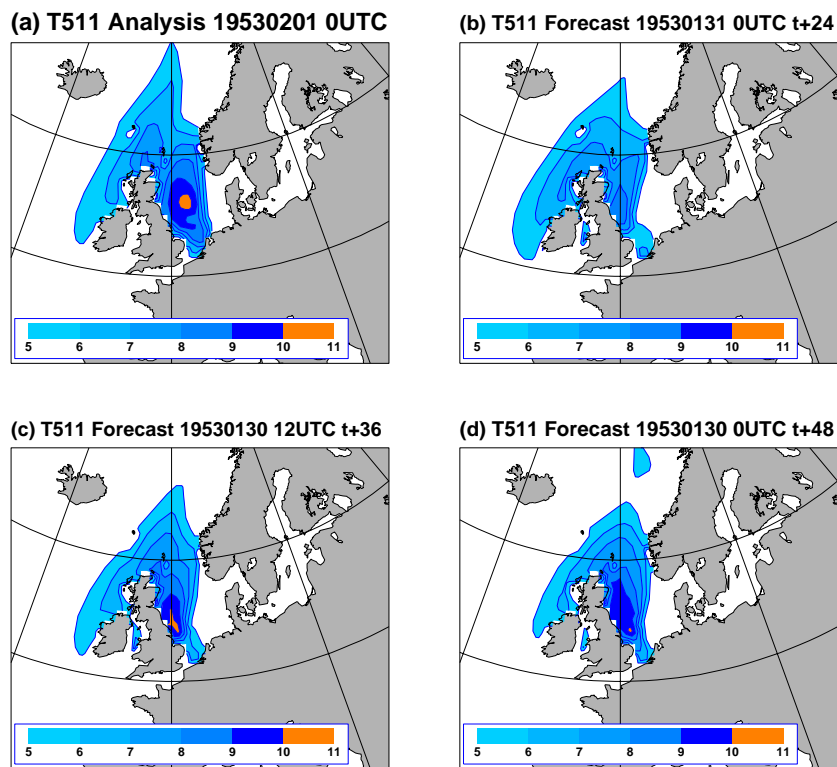


Figure 7: Significant wave height (m) for the (a) the analysis and (b) 24, (c) 36, and (d) 48 hour forecasts verifying at 00 UTC 1 February 1953.

3.3 Ensemble Forecasts

The deterministic forecasts show a good indication of disastrous wind speeds in coastal areas of East Britain and the Netherlands up to 48 hours ahead. Now, the question arises whether the ensemble prediction system would have supported such an early warning and, moreover, whether the warning period available to the authorities could have been extended using information from the ensemble.

From the ensemble the first indications for the possibility of a storm appear at a forecast range of 108 hours when about 10 members out of a total of 50 show a larger pressure gradient in the North Sea than the T511 deterministic forecast (Fig. 8). However, the maximum gradient in these forecasts is generally too far to the north, similar to the behaviour of the 72 hour deterministic forecast.

At a forecast range of 84 hours almost 50% of all the members of the ensemble produce a rather large pressure gradient over the North Sea and some of them come close to the analysed pattern of the mean sea level pressure (Fig. 9). There is, however, still the tendency to move the area of the largest gradient too far to the north.

This picture changes noticeably as the forecast range comes closer to the storm event (Fig. 10). Almost all members of the perturbed 60 hour forecast ensemble support the control forecast and the high resolution T511 forecast by producing a deep surface low in the area of interest. Though there is still the tendency of having the largest gradient too far to the north, there are at least 10 members which indicate that the strong pressure gradient would extend to coastal areas of the Netherlands. The fact that almost all ensemble members produce a major storm 60 hours in advance shows that the sensitivity of this storm to small analysis uncertainties is rather small. This is an important information in the context of severe weather prediction for it provides confidence in the forecast.

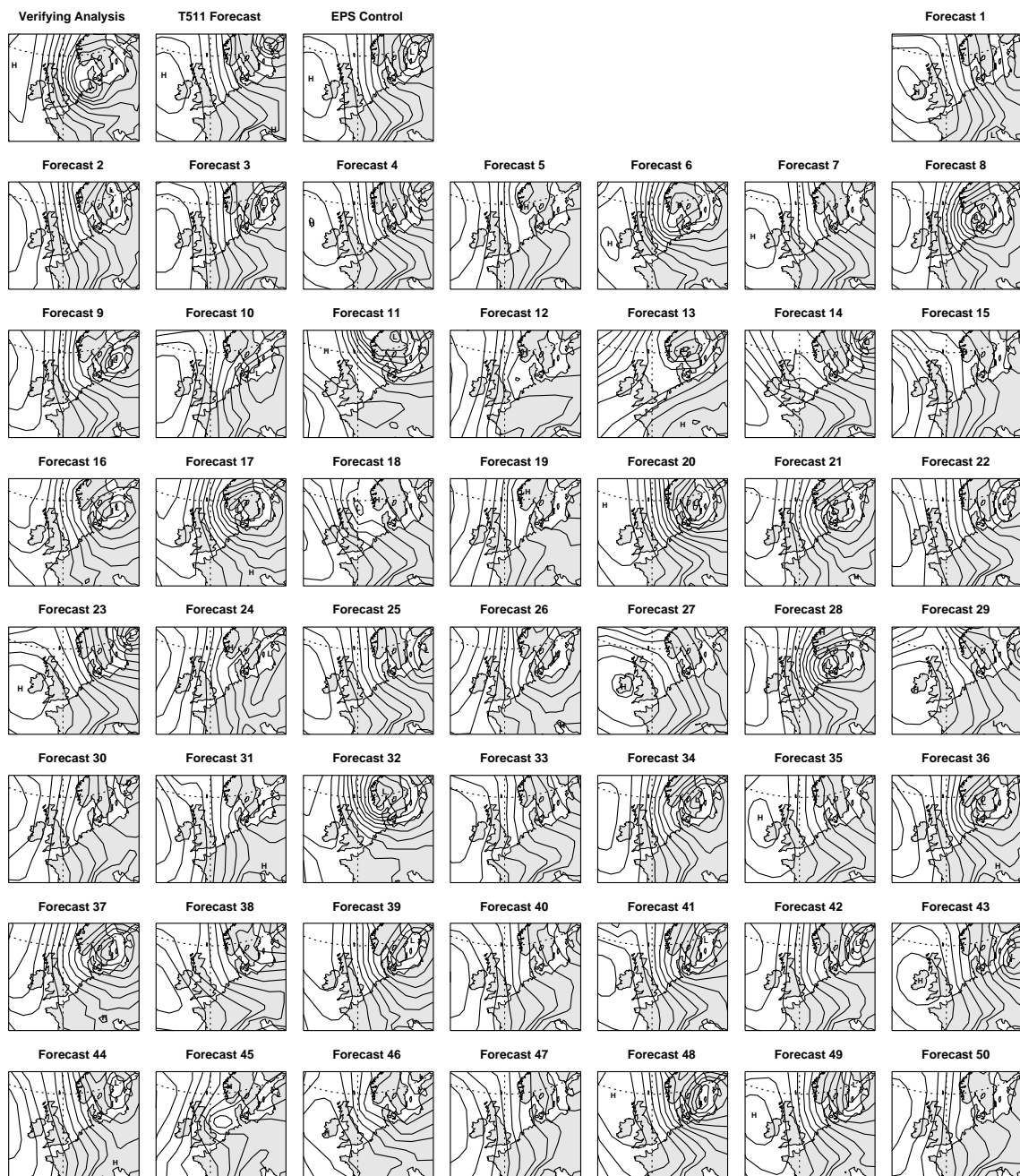


Figure 8: Verifying mean sea level pressure analysis (hPa) at 00 UTC 1 February 1953 (upper left panel) along with corresponding 108 hour forecast started at 12UTC 27 January 1953. Shown is the deterministic T511 forecast, the EPS control forecast, and 50 members of the ensemble (Forecast 1–50). Contour interval is 5 hPa.

It is interesting to investigate the 36-hour ensemble (Fig. 11) with respect to the location of the cyclone. As in the short-range deterministic forecast for both resolutions, T255 and T511, most of the ensemble members have a cyclone of smaller spatial scale than the analysed one and being located slightly south-east of the analysed cyclone with the important implication, that a large part of the maximum pressure gradient is over land rather than over sea. Despite those shortcomings, at this forecast range the ensemble prediction system would still give the basis for a definite warning of a major storm to come.

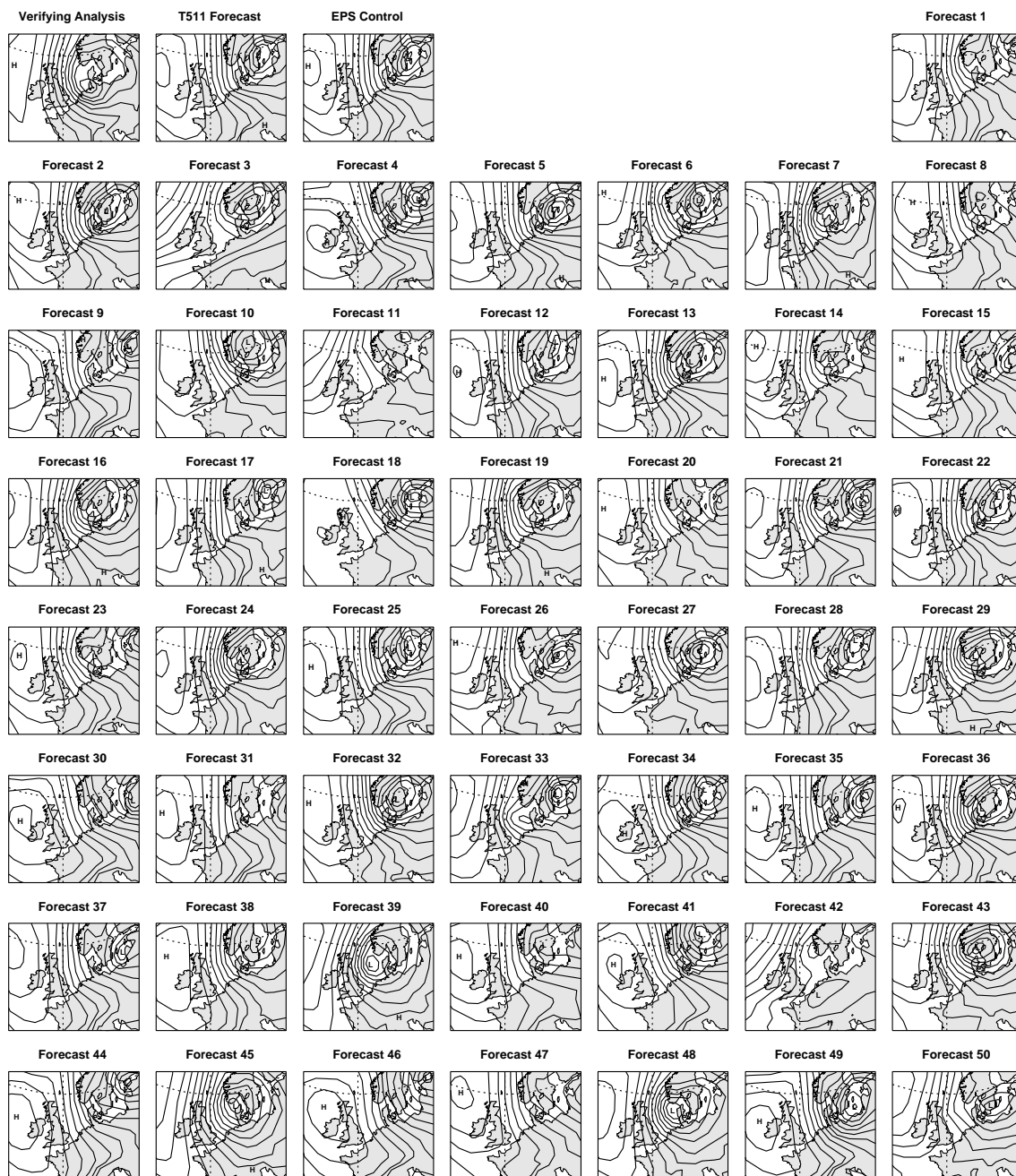


Figure 9: As in Fig. 8 except for 84 hour forecasts started at 12UTC 28 January 1953.

The probability distribution of gustiness effectively summarizes the performance of the EPS in predicting the storm for different forecast ranges (Fig. 12). By selecting a threshold value of 29 m/s (11 Bft) the probability distribution in the short-range (36 hours, right panel in Fig. 12) resembles fairly well the deterministic T511 forecast of gustiness (Fig. 6). Extending the forecast range to 60 hours (Fig. 12 middle panel) has two effects. It broadens the area of high probabilities and, more significantly, reduces the probability in south-western parts of the North Sea. A further 24-hour extension of the forecast range reduces the probability of strong winds even further close to the Dutch coastline with the highest probabilities now found in northern parts of the North Sea. The probabilistic forecast for the north-western North Sea, thus, is still quite skilful even 84 hours in advance!

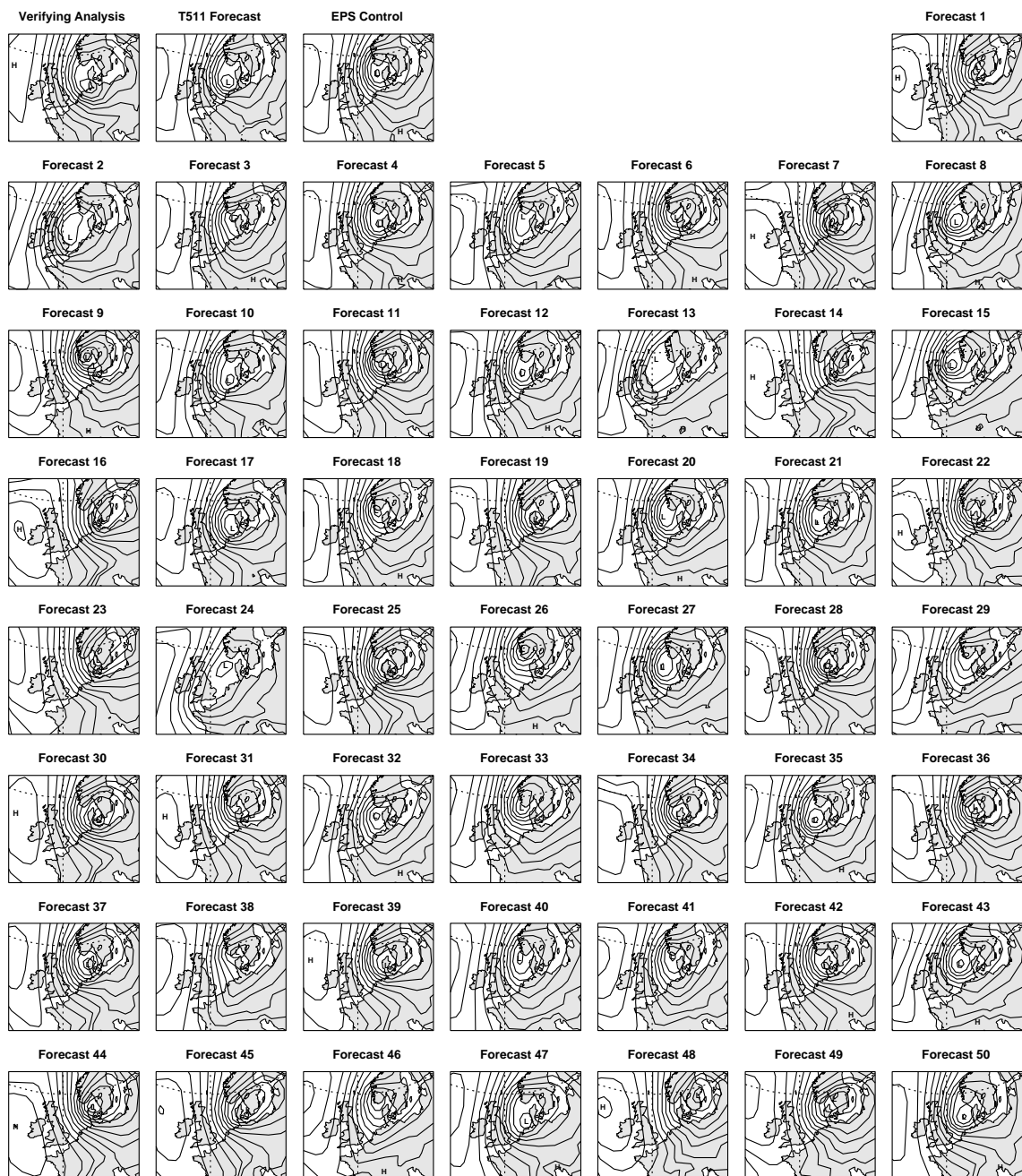


Figure 10: As in Fig. 8 except for 60 hour forecasts started at 12UTC 29 January 1953.

4 The Hamburg storm of 17 February 1962

The next severe European storm of the 20th century considered in this study occurred during the night from 16 to 17 February 1962. A cyclone split into two parts at the southern tip of Greenland; one moved north along the west coast of Greenland while the other one moved into the Norwegian Sea. The eastward moving cyclone was named Vincinette (the invincible) before it was known that this cyclone would develop into a powerful cyclone accompanied by gale force winds causing wide spread damage and creating a surge large enough to flood wide

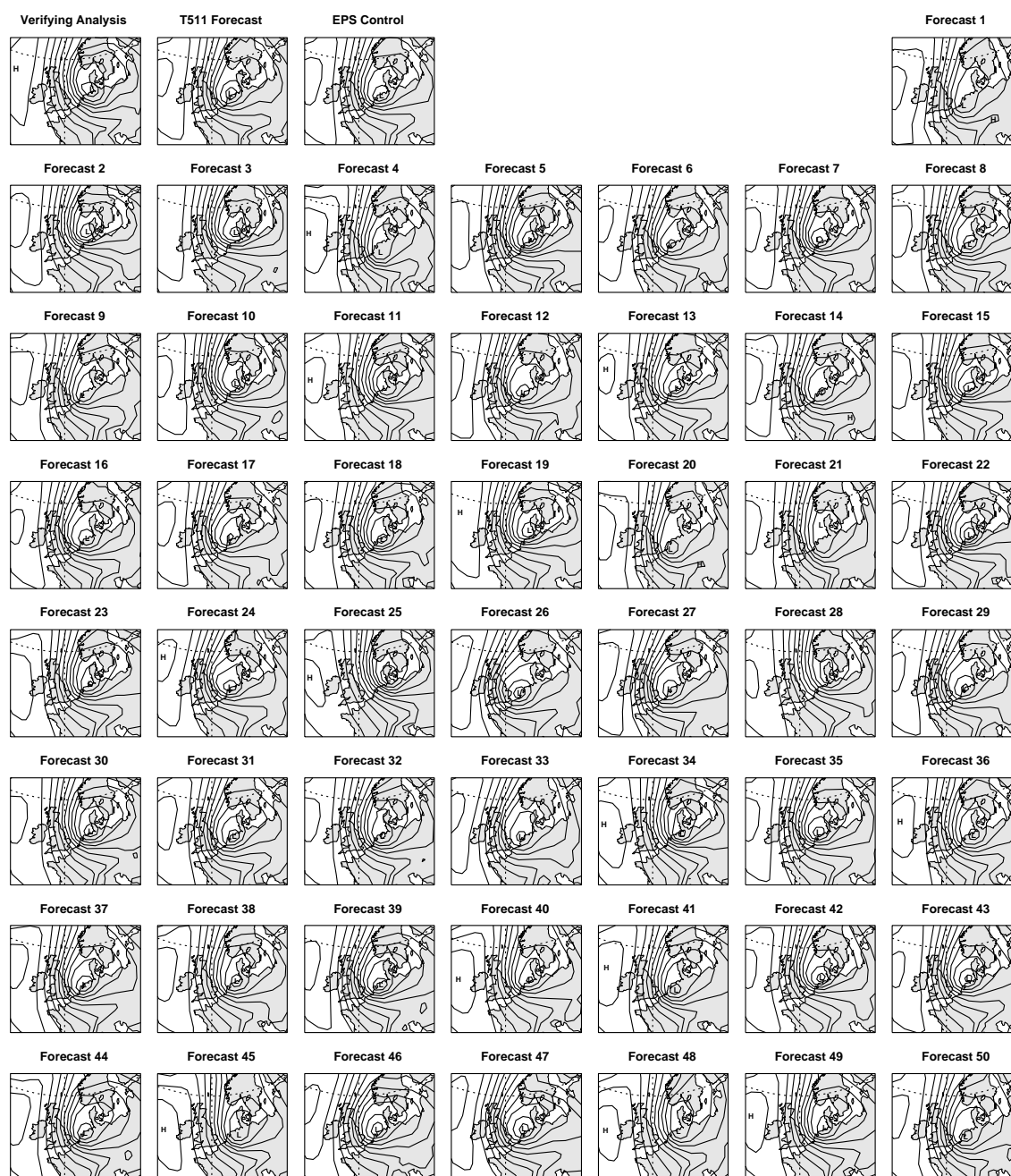


Figure 11: As in Fig. 8 except for 36 hour forecasts started at 12UTC 30 January 1953.

areas of the city of Hamburg 70 km upstream the mouth of the river Elbe. The dykes broke at 60 places leading to floods that killed 340 people.

4.1 Evolution of the storm

Similar to the 1953 storm the evolution of a deep depression caused an enormous pressure gradient over the North Sea. In this case, however, the cyclone moved from Iceland over Norway into a more easterly position

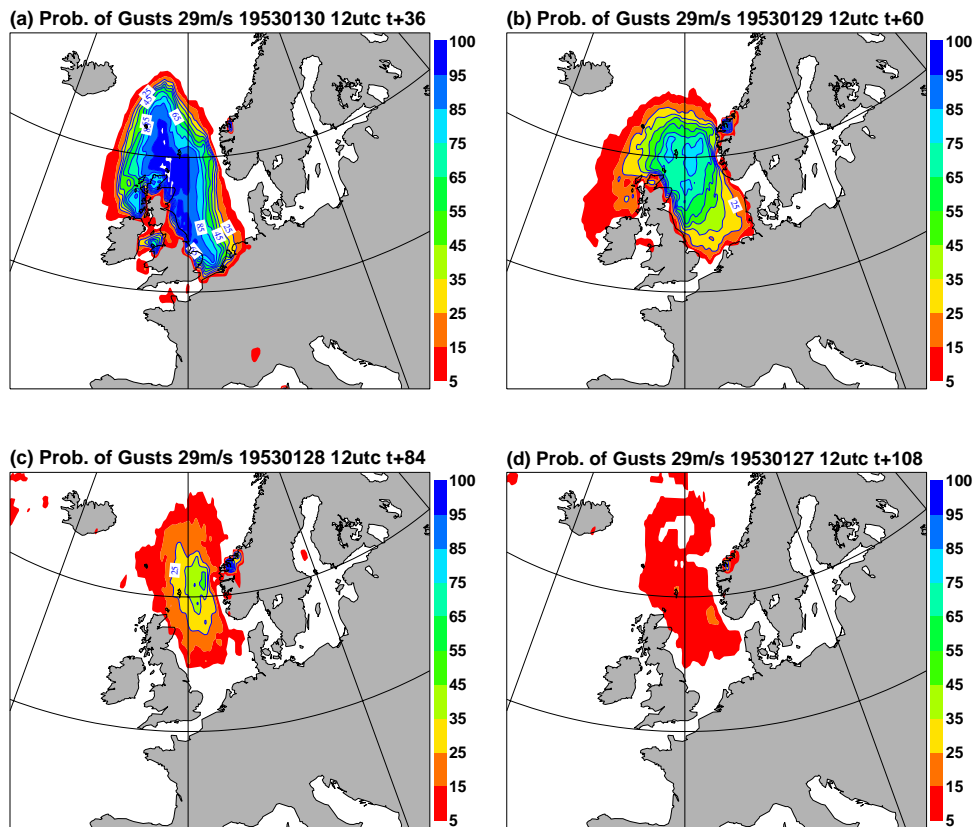


Figure 12: Probability (%) of maximum wind gusts exceeding 29 m/s (11 Bft) for (a) 36, (b) 60, (c) 84, and (d) 108 hour ensemble forecasts verifying at 00 UTC 1 February 1953. The probabilities have been estimated using the control forecast along with 50 perturbed ensemble members.

over Sweden and the Baltic Sea (Fig. 13) leading to strongest winds in central and south-eastern parts of the North Sea. The fairly large-scale cyclone deepened to an extremely low central pressure of 953.1 hPa. Associated gale force north-westerly winds with gust of more than 33 m/s (12 Bft) moved from the North Atlantic into the North Sea, with the largest wind speed found in the German Bight during the night from 16 to 17 February 1962.

Similar to the Dutch storm Vincinette was of relatively large spatial scale and the period of gale force winds in south-eastern parts of the North Sea was rather extensive (longer than 12 hours). In the first detailed description of the storm published in the “Berliner Wetterkarte” about one month after the catastrophe took place, Scherhag highlighted this fact while putting Vincinette into a historical context (Scherhag, 1962).

4.2 Deterministic Forecasts

As part of the cyclogenesis a deep upper air low developed over the Baltic Sea with a strong south-west/north-east pressure gradient covering the entire North Sea (Fig. 14 upper left panel). In the short-range (D+1 and D+2 forecasts) all major features seen in the analysis are well predicted. In the D+3 forecast there is a tendency to weaken the gradient in eastern parts of the North Sea.

At D+4 and D+5 the main north-westerly flow is still the dominant feature; the northerly wind component,

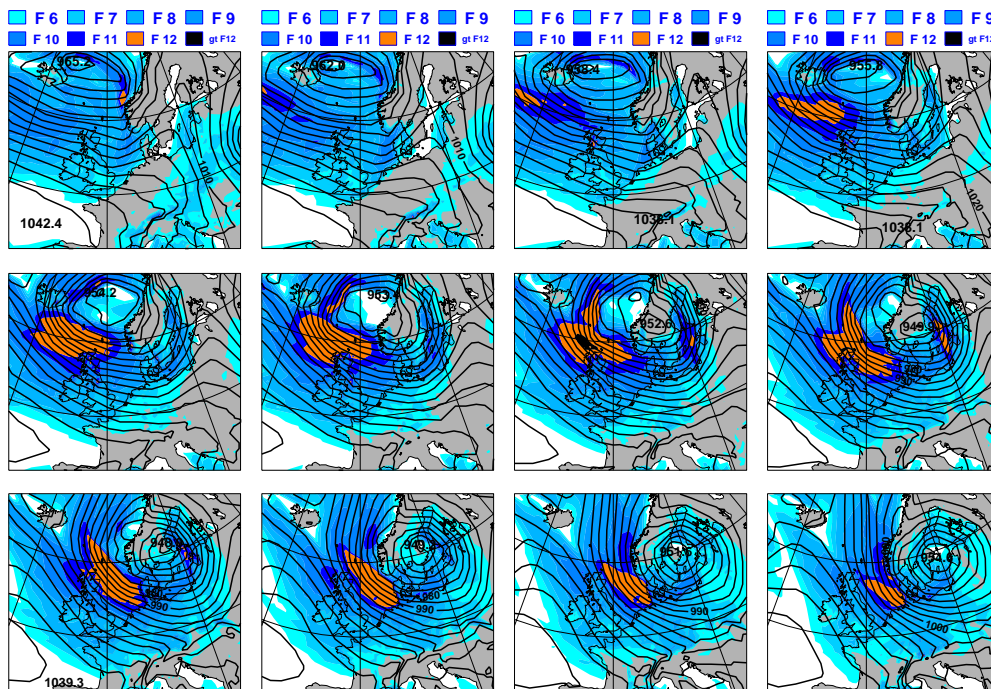


Figure 13: Mean sea level pressure (contours in hPa) and maximum wind gusts (shading in Bft) for intervals of 3 hours from 15 UTC 15 February 1962 (upper left panel) to 00 UTC 17 February 1962 (lower right panel).

however, is much reduced though the horizontal pressure gradient is even larger than in the analysis (Fig.17). A clear sign of loss of predictive skill is seen beyond D+4 with too weak gradients over the North Sea.

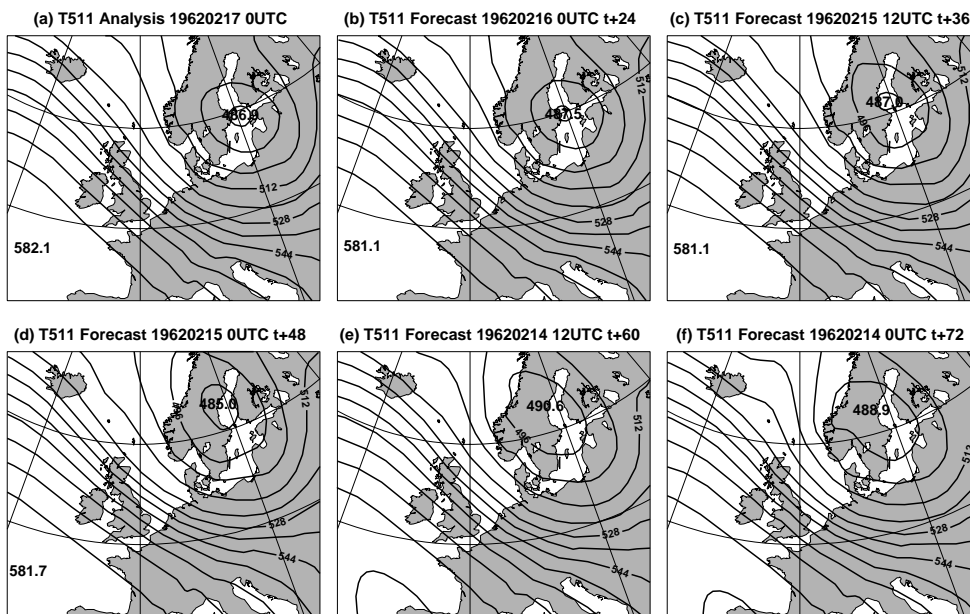


Figure 14: (a) 500 hPa geopotential height analysis (dm) along with corresponding short-range forecasts all verifying at 00 UTC 17 February 1962: (b) 24, (c) 36, (d) 48, (e) 60, and (f) 72 hour forecasts.

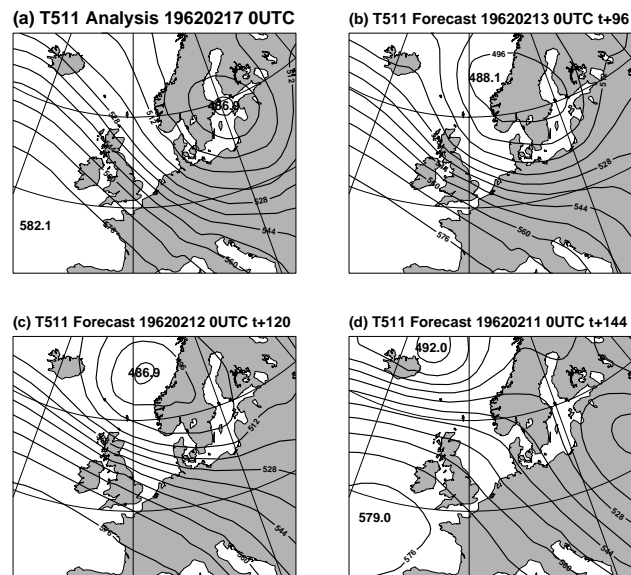


Figure 15: As in Fig. 14, except for medium-range forecasts: (b) D+4, (c) D+5, (d) D+6.

For the low level flow we compare the high-resolution 4D-VAR analysis (T511) with the low resolution 3D-VAR (T159) analysis that has been run as an ERA-stream together with low-resolution forecasts based on model cycle 23r4 in ERA-40-type configuration (Fig. 17).

Though the cyclone has an extremely low central pressure of 953.1 hPa in the high resolution analysis, the fairly large scale pattern of the cyclonic system probably helps the low resolution analysis to produce an almost

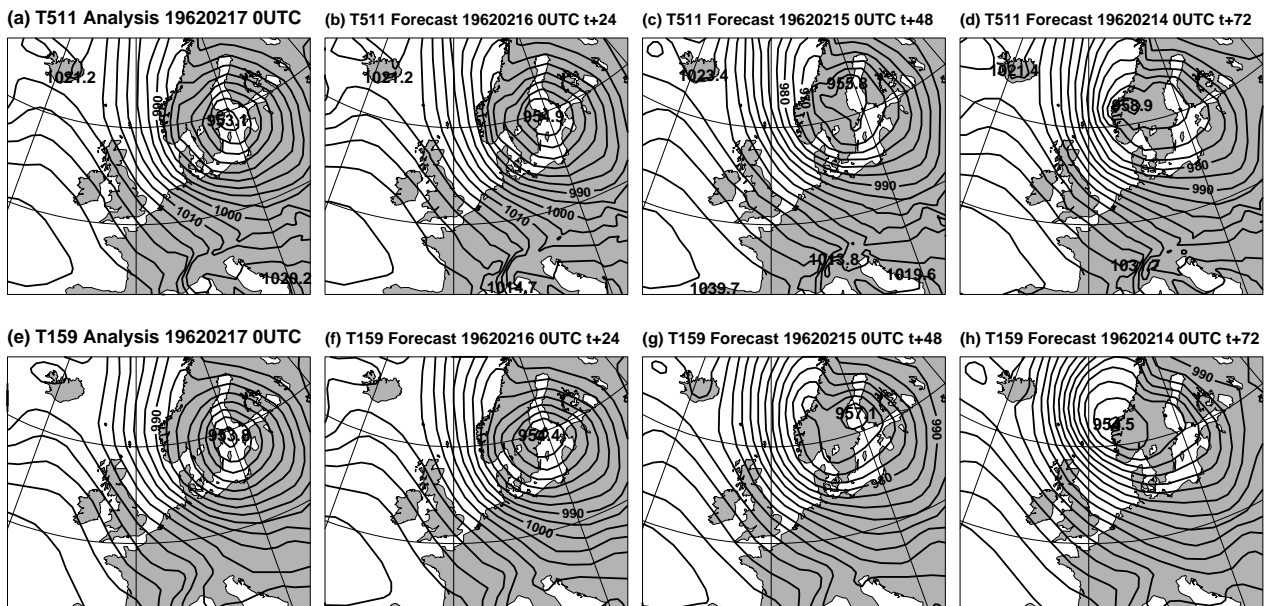


Figure 16: Mean sea level pressure field (hPa) for the analysis and short range forecasts verifying at 00 UTC 17 February 1962: (a) analysis along with (b) D+1, (c) D+2, and (d) D+3 forecast using the T511 system based on model cycle 25r4; (e) analysis along with (f) D+1, (g) D+2, and (h) D+3 forecasts using the ERA40-type T159 system based on model cycle 23r4.

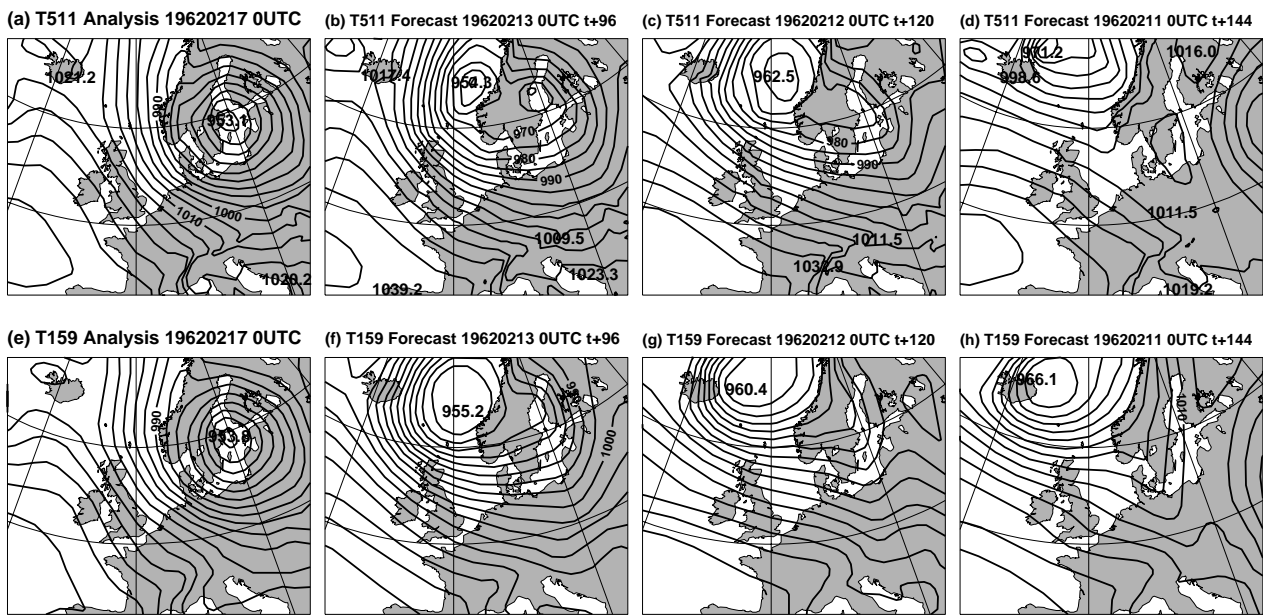


Figure 17: As in Fig. 16, except for medium-range forecasts: D+4, D+5, and D+6.

identical surface low with a central pressure of 953.8 hPa (only 0.7 hPa more than for the T511 analysis). The performance of the two systems in the short-range is almost identical; both predicting the maximum pressure gradient to be over the German Bight, and it was this gradient which led to the superposition of a big wind surge over the tidal wave⁴. Only at 72 hours differences between the high-resolutions and low-resolution forecasts appear that may have had direct consequences for possible storm warnings, with the low-resolution system showing a much weaker surface pressure gradient over the German Bight.

In the medium-range (D+4 and D+5) the main cyclone is located over the Norwegian Sea rather than over the Baltic Sea (Fig. 17). In the German Bight this forecast error is associated with a reduced surface pressure gradient and a stronger westerly component of the flow, the latter reduces the threat of flooding in the mouth of the river Elbe considerably. The D+6 forecast gives no indications whatsoever for a major storm event to influence the German Bight.

The MSLP and Z500 fields discussed above show that the analyses and deterministic forecasts skill for the Hamburg storm hardly depend on the horizontal resolution used (T159 versus T511). Similar results are found for the anomaly correlation skill score of Northern Hemisphere 500 hPa geopotential height fields shown in Fig. 18. The scores are based on data from the period 10 February to 19 February 1962 (10 days). There is a noticeable extension of predictability from 6 days to about 9 days (based on 60% anomaly correlation) when the latest model cycle 25r4 is used instead of the older cycle 23r4. While somewhat hampered by the limited number of cases, the improved performance of the latest model cycle is consistent with results for more recent periods (Andersson et al., 2003). We note in passing that the skill of the forecast is very good, well into the medium-range, which may be surprising given that only conventional data were available in 1962.

The differences between the high-resolution and low-resolution forecasts become apparent when we consider a parameter like gustiness which is more sensitive to resolution (Fig. 19). Whereas the T511 system produces gusts of 12 Bft in a broad band in the analysis and in the short-range forecast, the low-resolution system underestimates the gustiness in the North Sea by 1 Bft. Characteristic for the low-resolution system is also that

⁴It can be seen as a fortunate circumstance that the high tide during the night from 16 to 17 February took place two days before full moon, since it is two days *after* full moon that the highest tidal waves occur in the German Bight

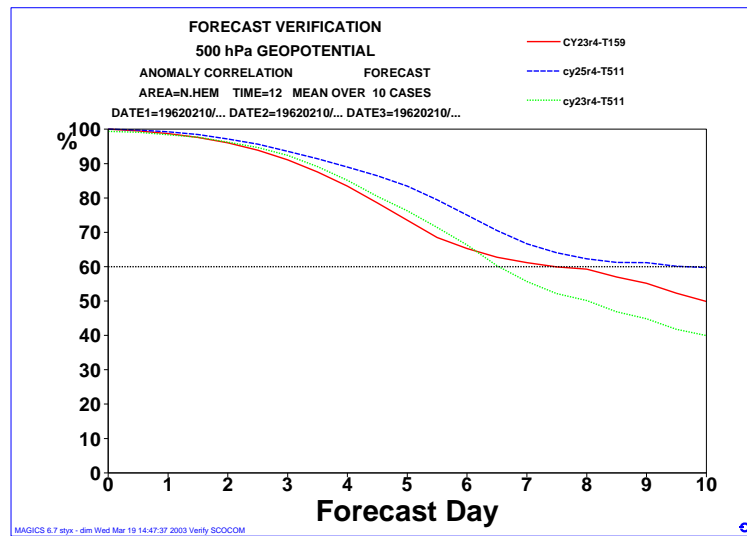


Figure 18: Anomaly correlation between analyzed and forecast Northern Hemisphere 500 hPa height fields: Low-resolution T159 ERA40-type system (red line), high-resolution T511 system based on model cycle 23r4 (green dashed line) and on model cycle 25r4 (blue dashed line).

it overestimates gusts over the Norwegian mountains and parts of the Alps as well. This might be due to the effect of the reduced orographic height in the low-resolution system.

Further, the T511 system produces a reasonable surface wind field up to 84 hours ahead (Fig.20). However, the area of extreme gale force winds (12 Bft and more) in the 60 and 84 hour forecast is much larger than in the analysis. As a result of this the forecast significant wave height, for example, is considerably overestimated. In

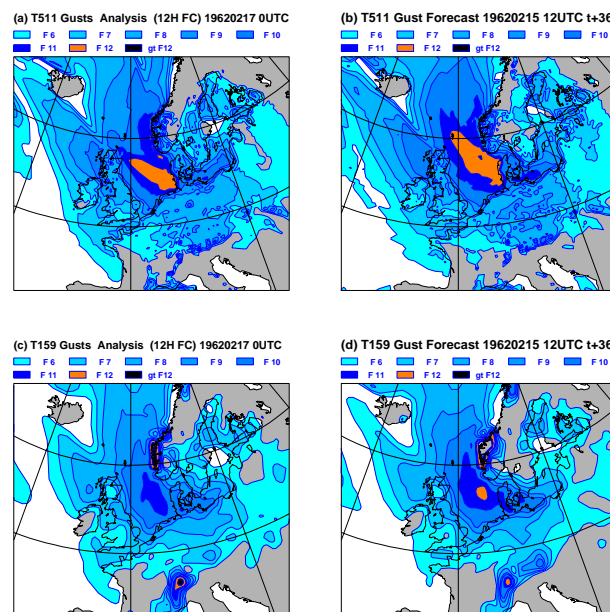


Figure 19: Maximum gusts (Bft) for the “analysis” (12-hour forecast) and 36 hours forecasts verifying at 00 UTC 17 February 1962: (a)–(b) high resolution T511 system based on model cycle 25r4 and (c)–(d) low-resolution T159 ERA40-type system based on cycle 23r4. The gustiness represents maximum gusts during the last 12 hours of the forecast.

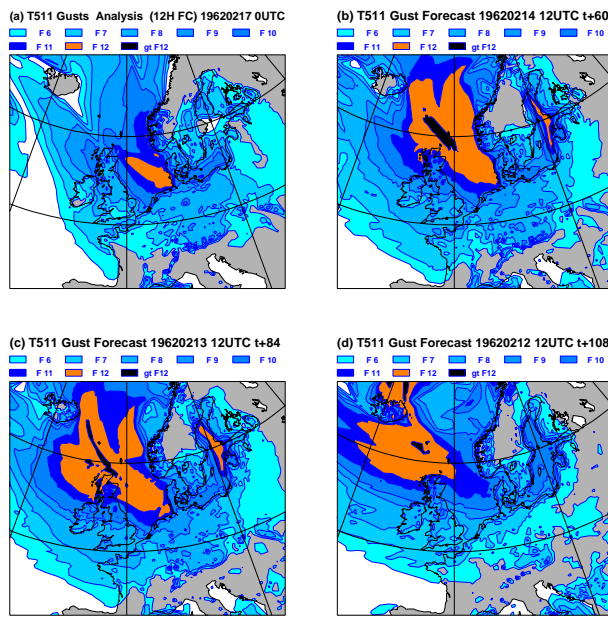


Figure 20: Maximum gusts for the (a) analysis (12-hour forecast) and (b) 60, (c) 84, and (d) 108 hours forecasts verifying at 00 UTC 17 February 1962. Analysis and forecasts are based on the high-resolution model (T511) cycle 25r4.

the 36 to 84 hour forecasts the significant wave heights are larger by up to 3 meters compared to the analysis (Fig. 21). At 108 hours the maximum gusts in the German Bight are so strongly underestimated that a storm surge warning presumably would not have been given.

Summarizing, the deterministic forecast provides evidence of north-westerly gale force winds (12 Bft) in south-

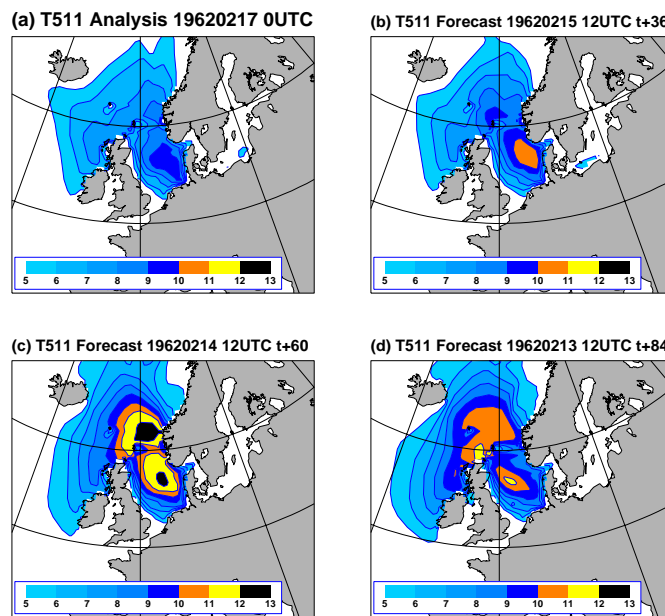


Figure 21: Significant wave height for the (a) analysis and (b) 36, (c) 60, and (d) 84 hour forecasts verifying at for the 00 UTC 17 February 1962. Analysis and forecasts are based on the high-resolution model (T511) cycle 25r4.

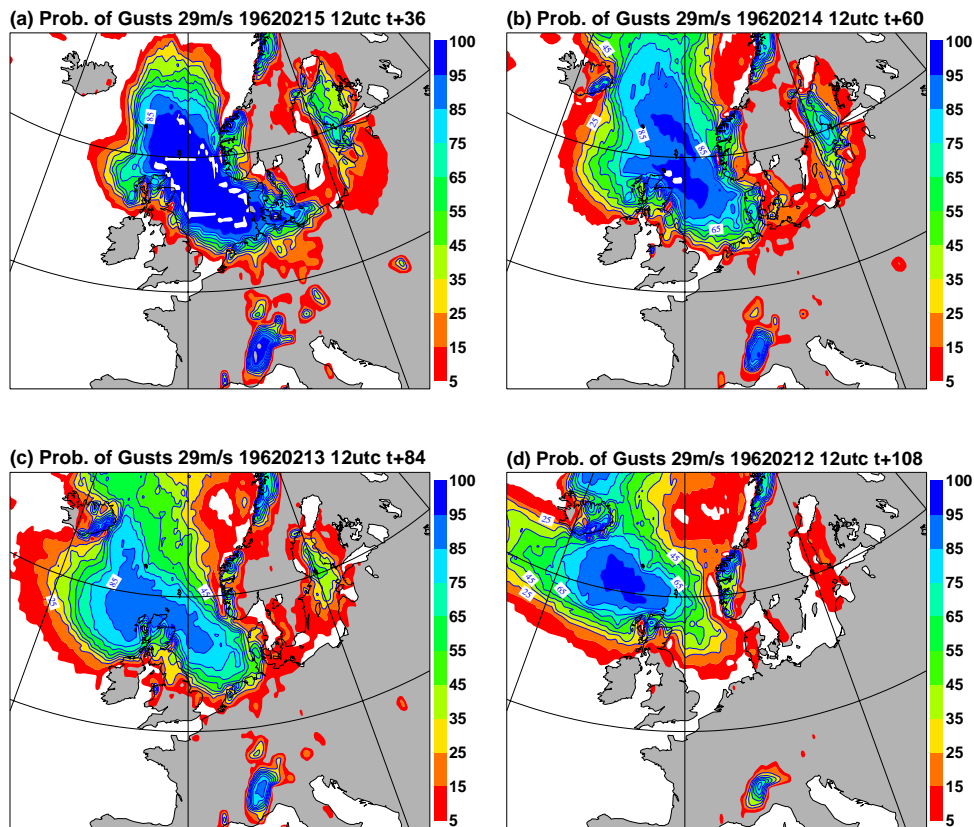


Figure 22: Probability (%) of maximum gusts greater than 29 m/s (11 Bft) for (a) 36, (b) 60, (c) 84, and (d) 108 hour forecasts verifying at 00 UTC 17 February 1962. Probability estimates are based on the control forecast and all 50 ensemble members.

western parts of the North Sea as early as 84 hours in advance.

4.3 Ensemble Forecasts

The EPS has been run from initial conditions up to 108 hours in advance of the major storm event. At the forecast range of 108 hours all ensemble members follow fairly closely the T511 forecast and the T255 control forecast by predicting strong winds (not shown) mainly in northern parts of the North Sea and the North Atlantic. Only two ensemble members show strong gusts in the German Bight at 108 hours. For the 84 hour ensemble forecast the picture is completely different (not shown). More than 50% of all ensemble members extend the strong wind field into the German Bight, thereby confirming the threat of a dangerous storm surge for the mouth of the river Elbe. The ensemble clearly overestimates maximum gustiness in the north-eastern North Atlantic.

The probability of gusts exceeding 29 m/s (11 Bft) is shown in Fig.22 for four different forecast ranges (36, 60, 84, and 108 hours). For all forecast ranges the areas with highest probabilities coincide with gustiness maxima of the corresponding deterministic forecast (see Fig. 19 and 20). The EPS shows no indication for gale force winds in the German Bight 108 hours in advance. The probability for gusts exceeding 11 Bft in the German Bight amounts to about 50% for the 84 hour ensemble; 36 hours in advance the probability has increased to more than 90%. From the ensemble forecasts it is clear that reliable warnings could have been issued by as

much as 84 hours in advance!

5 The Storm of 15/16 October 1987

The final storm to be described is the Great Storm which hit south-east England and north-west France during the night 15–16 October 1987. In a narrow band from north-west France to south-east England the strongest gusts exceeded 50 m/s. [Burt and Mansfield \(1988\)](#) estimated the return period for such gusts to be longer than 200 years⁵! In England and France 20 people lost their lives as a result of the gales. Furthermore, the gales led to damages worth hundreds of million of pounds.

The operational forecasts of the Great Storm gave good guidance in the medium-range ([Morris and Gadd, 1988](#); [Jarraud et al., 1989](#)). On Sunday 11 October, for example, the then operational models predicted a storm to occur in south England and north-west France late on Thursday 15 October 1987 ([Morris and Gadd, 1988](#)). Further, throughout the medium-range the forecasts have been quite consistent. In the short-range, though, there has been little guidance through operational forecasts in terms of the track, location and intensity of the storm.

In this study the predictability of the Great Storm in the short-range and medium-range is revisited using the most recent version of the ECMWF forecasting system. In the short-range we focus on the question whether the usage of the latest (4dVar) data assimilation scheme and forecast model would have improved the poor operational forecasts. In the medium-range emphasis will be on results from the EPS.

5.1 Evolution of the storm

During the days preceding the Great Storm, a deep trough of low pressure was located over the eastern North Atlantic. On its eastern flank, warm and moist air of subtropical origin was advected as far as north-east Europe giving rise to very pronounced low-level baroclinicity ([Hoskins and Berrisford, 1988](#)). Precursors of the Great Storm appeared during the night 14/15 October west off the north-western coast of Spain. From there the storm moved within the next 24 hours under rapid intensification (about 35 hPa in 24 hours) towards southern England (for details, see [Morris and Gadd, 1988](#); [Burt and Mansfield, 1988](#)).

The evolution of the storm in terms of mean sea level pressure (MSLP) and maximum gustiness is shown in [Fig. 23](#) for the period from 15 UTC 15 October to 12 UTC 16 October. Notice, that the upper (lower) row is based on very short-range 3, 6, 9, and 12 hour forecasts started from 12 UTC 15 October (00 UTC 16 October). From the very poor short-range forecast started at 12 UTC 15 October ([Fig. 23](#), upper row) there is little indication for the pronounced deepening of the low pressure system. The forecast MSLP over southern England and north-west France at 00 UTC 16 October is about 970 hPa compared to analyzed values of about 960 hPa ([Fig. 24a](#)) and MSLP gradients are much weaker in the forecast compared to those from the analysis. The poor short-range forecast, therefore, makes it difficult to describe the development of the storm in terms of parameters like maximum gustiness which are based on short-range model integrations. The short-range forecast started at 00 UTC 16 October is much more skilful and can be used to describe the evolution of the storm during its mature phase ([Fig. 23](#), lower row). Evidently, the band of maximum gustiness during the first half of 16 October extends from the Channel, through south-east England into the North Sea, a feature that is in good agreement with the observations (e.g., [Burt and Mansfield, 1988](#)).

⁵Note, though, that France was hit by gusts of similar intensity only 12 years later during the Christmas storms in 1999.

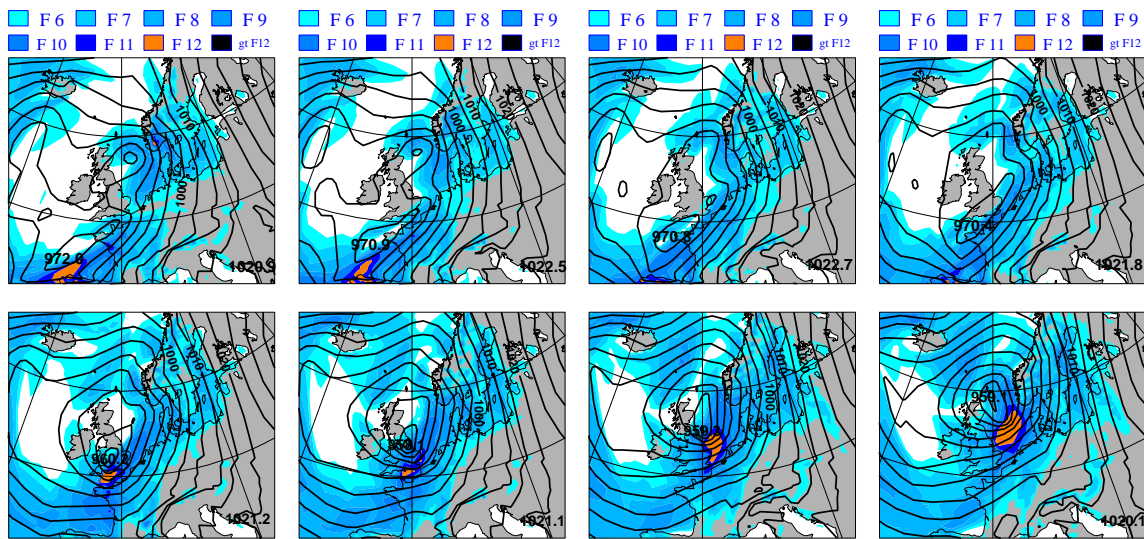


Figure 23: Mean sea level pressure (contours in hPa) and maximum gusts (shading in Beaufort) for intervals of 3 hours from 15 UTC 15 October (upper left panel) to 12 UTC 16 October 1962 (lower right panel). Notice, that the values are forecast (3, 6, 9, and 12 hour forecasts from left to right)!

5.2 Deterministic Forecasts

Short-range deterministic forecasts using the high-resolution model (cycle 25r4) are shown in Fig. 24 for the target dates 00 UTC 16 October (upper row) and 12 UTC 16 October. As for the operational forecasts from 1987 (see Morris and Gadd, 1988; Jarraud et al., 1989, for details) the very short-range forecast from 12 UTC 15 October (Fig. 24b,f) based on the latest ECMWF system underestimates the severity of the storm 12 and 24 hours later. The forecasts started earlier (12 UTC from 14 to 12 October) all show the occurrence of a major storm event in the region of interest. With increasing lead time, however, the forecast north-eastward progression of the storm becomes slower and slower amounting to a phase error of about 12 hours for the 84 and 96 hour forecasts started at 12 UTC 12 October (Fig. 25). Beyond 96 hours the deterministic forecast provides little evidence for the occurrence of a major storm over southern England and north-west France.

In summary, the latest ECMWF system gives improved short-range and medium-range deterministic forecasts for the Great Storm of October 1987 compared to the then operational system. However, one of the major problems of forecasting the Great Storm, that is, the “loss” of the storm in 12 and 24 hour forecasts started at 12 UTC 15 October, is only slightly improved and certainly not resolved by using the latest ECMWF forecasting system.

All deterministic forecasts described above were started from analyses that are based on conventional data only, that is, no satellite data have been used. We have re-run T511 forecasts based on the latest model cycle 25r4 using ERA-40 data as initial conditions. In October 1987 ERA-40 used conventional data along with satellite data from the SSM/I, MSU and HIRS instruments. The high-resolution forecasts based on ERA-40 data are very similar to the forecasts based on conventional data only (not shown). In particular the poor forecast performance in the very short-range is not improved if satellite data are included. It should be kept in mind, though, that the ERA-40 reanalysis has been carried out at relatively low resolution (T159). This might be problematic in the context of the October storm, which was associated with relatively small-scale features and sharp gradients.

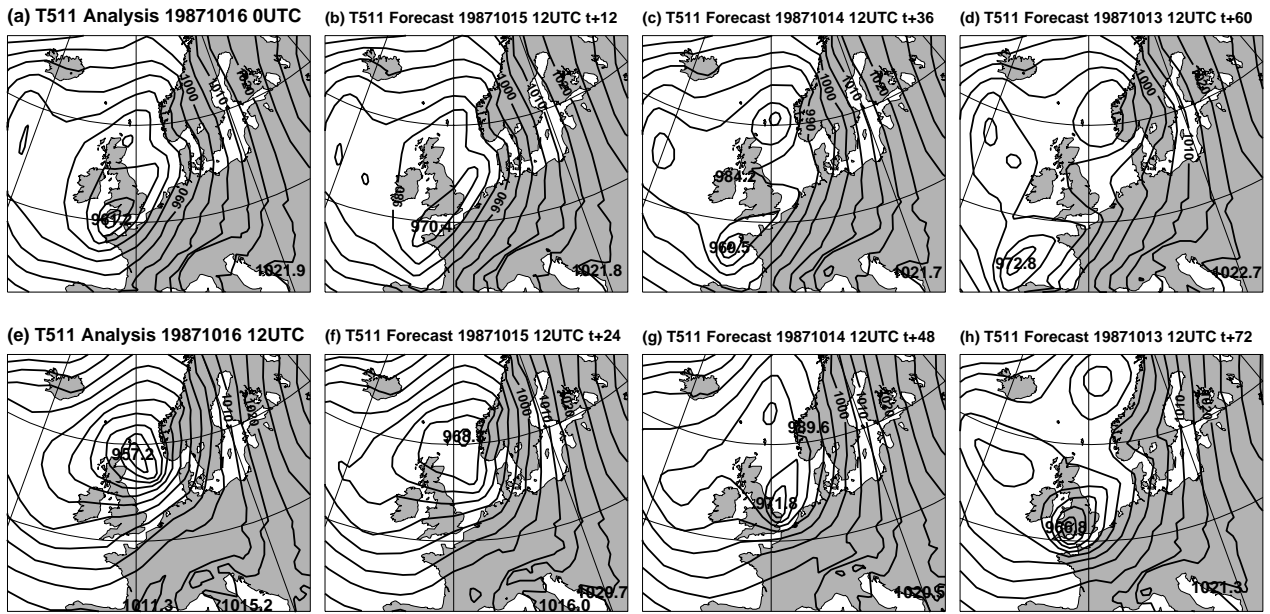


Figure 24: Mean sea level pressure field (hPa) based on the T511 model cycle 25r4 using non-satellite data only: (a) analysis and (b) 12, (c) 36, and (d) 60 hour forecasts verifying at 00 UTC 16 October 1987. (e) analysis, (f) 24, (g) 48, and (h) 72 hour forecasts verifying at 12 UTC 16 October 1987.

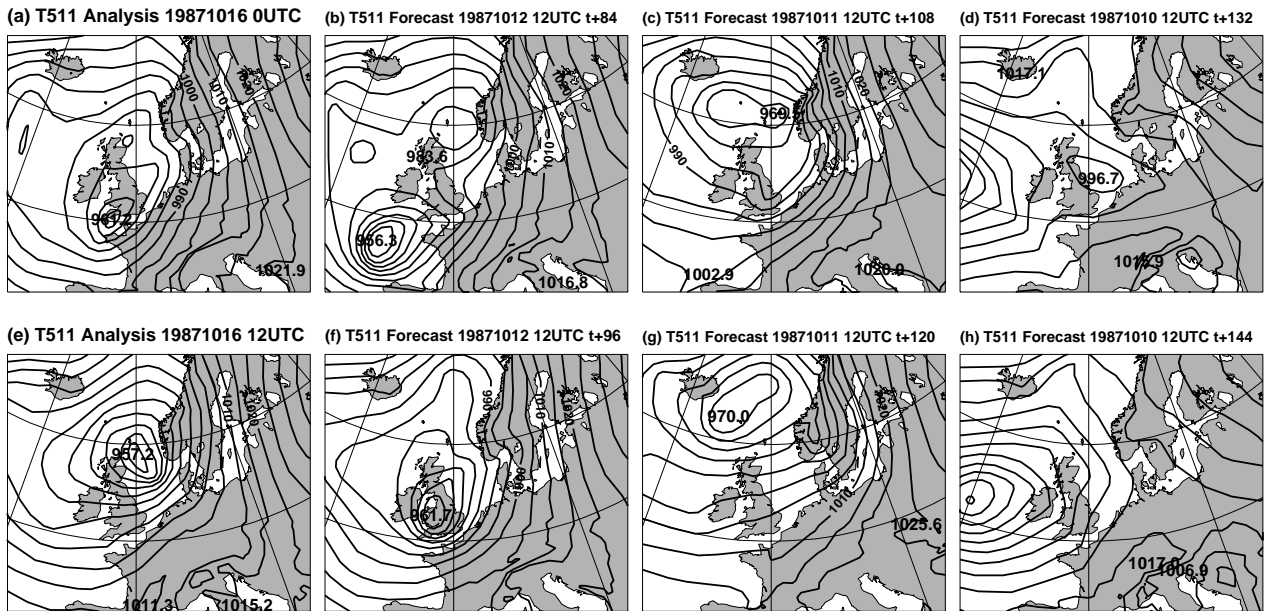


Figure 25: Mean sea level pressure field (hPa) based on the T511 model cycle 25r4 using non-satellite data only: (a) analysis and (b) 84, (c) 108, and (d) 132 hour forecasts verifying at 00 UTC 16 October 1987. (e) analysis, (f) 96, (g) 120, and (h) 144 hour forecasts verifying at 12 UTC 16 October 1987.

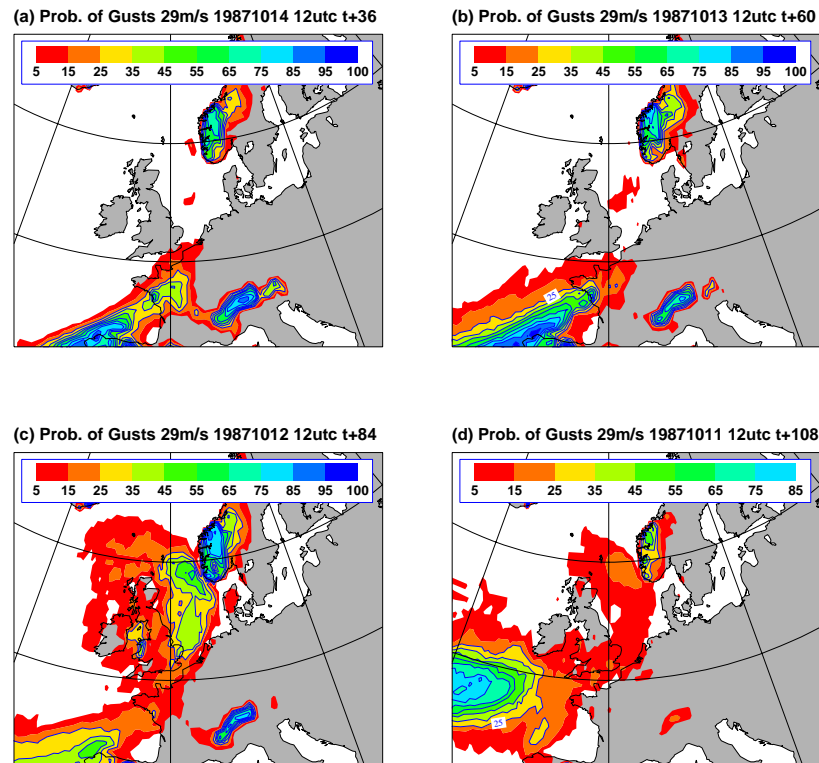


Figure 26: Probability (%) of maximum gusts exceeding 29 m/s (11 Bft) for (a) 36, (b) 60, (c) 84, and (d) 108 hour forecasts verifying at 00 UTC 16 October 1987. Probability estimates are based on the control forecast and all 50 ensemble members. Maximum values of gustiness are based on the 12 hour period 12 UTC 15 October to 00 UTC 16 October.

5.3 Ensemble Forecasts

Probability forecasts of maximum gustiness exceeding 29 m/s (11 Bft) for the period 12 UTC 15 October to 00 UTC 16 October 1987 are shown in Fig. 26. Thus, maximum gustiness values shown in Fig. 26 reflect the passage of the low pressure system from off the coast of north-west Spain towards south-west England explaining the band-like structure of the area high probabilities of maximum gustiness. Relatively high probabilities of up to 50% for maximum gusts exceeding 11 Bft can be found over north-west France 36 and 60 hours in advance. There is still a probability of about 10% in the Channel region 84 and 108 hours in advance. At this forecast range, however, highest probabilities are found in other regions (e.g., the North Sea at 84 hours).

Probability forecasts of maximum gustiness exceeding 29 m/s during the period 00 UTC to 12 UTC 16 October are shown in Fig. 27. During this period the storm moved from its position over southern England into the northern North Sea. Again, the narrow band-like structure reflects the fast movement of the storm within the 12 hour period. High probabilities are found 24, 48, and 72 hours in advance in regions that have been strongly affected by the storm. The ensemble, thus, gives relatively high confidence for the occurrence of gale force winds in a band from north-west France to the central North Sea. The 96 hour ensemble forecasts still show probabilities of 5–25% in the region directly influenced by the storm; at this forecast range, though, maximum probabilities are found over the Bay of Biscay, that is, south-west of the area of observed maximum wind gusts. This is consistent with the tendency of the storm to move too slowly for most of the individual ensemble members (not shown).

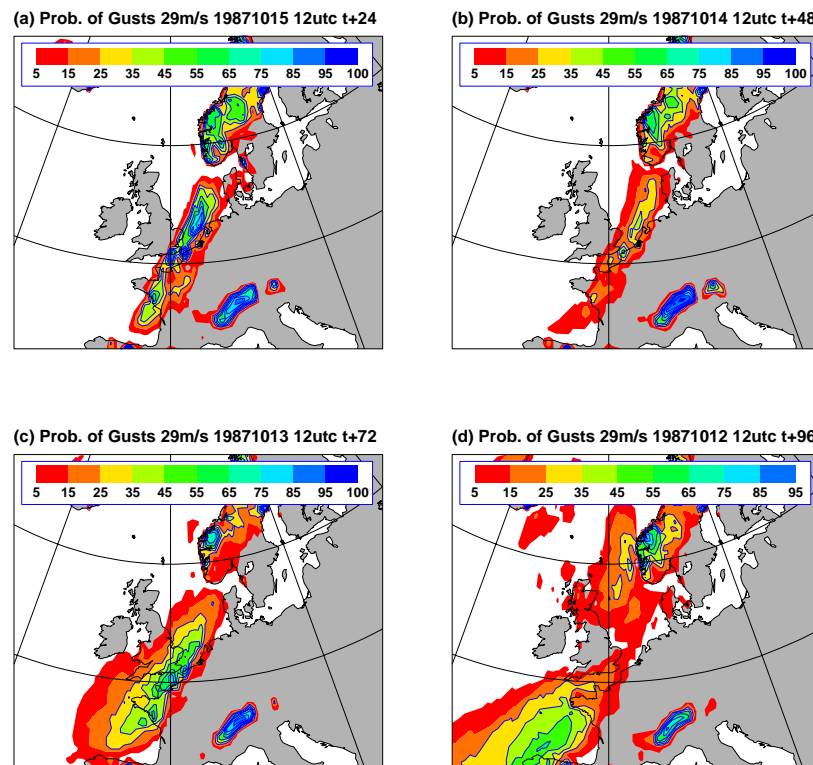


Figure 27: Same as in Fig. 26, except for (a) 24 hour, (b) 48 hour, (c) 72 hour, and (d) 96 hour forecasts verifying at 12 UTC 16 October 1987. Maximum values of gustiness are based on the 12 hour period 00 UTC 16 October to 12 UTC 16 October.

6 Discussion

Three major European storms of the 20th century were reanalyzed and reforecast using historical observational data together with recent cycles of the ECWMF integrated forecasting systems. Indications for the occurrence of these storms have been found well into the early medium-range.

At the first glance it might be surprising that the Dutch storm of 1953 and the Hamburg storm of 1962 are so well analyzed and forecast given that fewer observations were available than there are nowadays. Wind observations at the 500hPa level based on radiosonde observations are shown in Fig. 28 for the period 10–15UTC on 30 January 1953 (upper panel) and 30 January 2003 (lower panel). Obviously, the total number of radiosonde-based wind estimates is larger in 2003 than it was in 1953. However, most of the radiosondes on 20 January 2003 were launched over the European continent; there are only few radiosonde observations over the North Atlantic. This is in contrast to 1953 when ocean weather ships C, J, K, and L provided a good radiosonde coverage over the North Atlantic. The fact that the radiosonde network in 1953 seems not worse than that used in 2003 (at least upstream of Europe) may explain the skill of the ECMWF forecasting system in producing good analyses and forecasts of the major storms in 1953 and 1962.

While we hope that this study is of some historical interest, it should be stressed that it is also motivated by more practical aspects. It is essential, for example, to rigorously test the influence of changes to the forecasting system which is used operationally on a daily basis. Traditionally this has primarily been done by running the modified system (so-called experimental suites) for a limited period of consecutive days. Given the rareness of severe weather events, thus, relatively little has been known about the influence of these changes on the

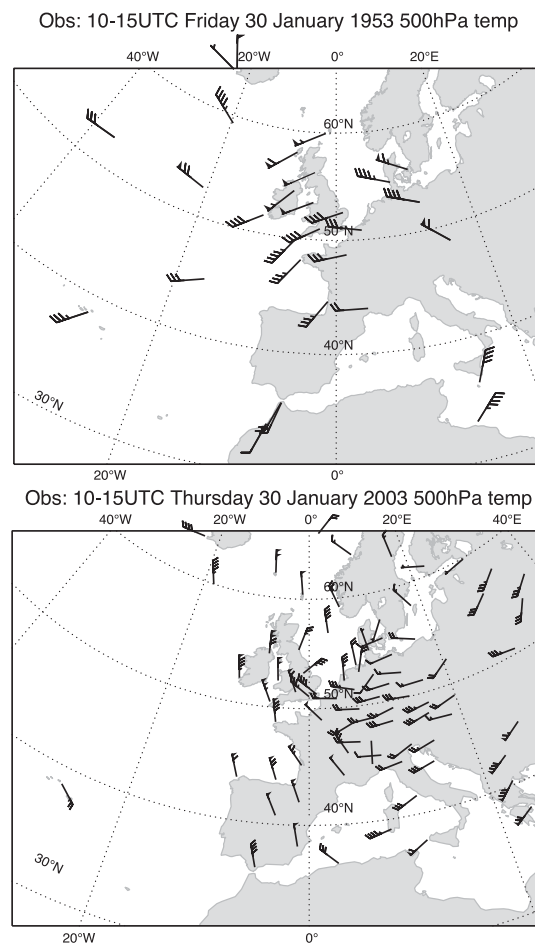


Figure 28: Radiosonde-based wind observations at 500hPa during the 5-hour window 10–15UTC: (upper panel) 30 January 1953 and (lower panel) 30 January 2003.

forecasts of severe weather events. In this context the results of this study can be seen as a reference against which future model cycles can be tested.

It is worth noting that it is the successful completion of the ECMWF Reanalysis Project (ERA-40) that has made the present study feasible. First, ERA-40 provides high-quality initial conditions covering the last 40 years which can be used for numerical experimentation. Second, the availability of archived observational data at ECMWF through ERA-40 allows to producing analyses with improved data assimilation systems for historical cases in a very efficient manner.

Another practical aspect of this study is that model assessment based on case studies like those presented above augment more abstract skill score-based evaluations and, thus, might well be of importance for routine users of operational forecast products—since it is the weather forecasters who have to issue early warnings based on numerical weather forecasting products. This is particularly true for *probabilistic* forecasts of severe weather events since ensemble forecasting is a relatively new technique with which not every forecaster might be familiar.

In fact, it has been shown for the cases described in this study that ensemble forecasts provide valuable additional information to single deterministic forecasts, that is, they allow to quantify the risk of the occurrence of severe weather. And it is the risk which is the crucial factor in decision making (Richardson, 2000). For all

three storms described the deterministic forecasts were quite skilful in the near medium-range. For these storms, therefore, the ensemble forecasts merely show that the probability of the deterministic forecast to be skilful is rather high. There might also be cases (or forecast ranges), though, where the deterministic forecasts fails to predict the storm whereas the ensemble indicates that there is some risk for the occurrence of a major storm. This can be seen, for example, for the Dutch storm in the medium-range for which the 108 hours deterministic forecast shows no storm in the North Sea, whereas the ensemble shows some members producing gale force winds in the North Sea (Fig. 8). Other examples of more recent storms are given by [Buizza and Hollingsworth \(2002\)](#).

It should be mentioned that the case studies presented in this study can not be seen as a rigorous assessment of the skill of severe weather prediction with the ECMWF forecasting system. First, any conclusions of the skill are hampered by the fact that only three cases were considered. Second, only one aspect has been considered, that is, the predictability of storms which actually turned out to happen. The other aspect, which is the occurrence of “false alarms” (a storm is forecast that does not occur), has not been addressed. Despite these short-comings, the successful prediction of three of the most extreme European storms of the 20th century well into the near medium-range with the latest ECMWF forecasting system shows that nowadays it is possible to perform reliable forecasts of wind storms several days in advance, thus, allowing early warnings to be issued to the public. This is particularly true since nowadays a much wider data coverage is available (e.g., through satellite data), which allows the initial conditions to be constrained much better.

Acknowledgements

We are grateful to Dave Burridge who was the initiator of this study. Comments by Tim Palmer and Adrian Simmons are acknowledged. We would also like to acknowledge the ERA-40 project, which has made it possible to study old cases and Jack Woollen from NCEP who made a special effort to correct and reformat the 1953 observations for the analysis of the Dutch storm. Rob Hine helped preparing Fig.28.

References

- Andersson, E., A. Beljaars, J. Bidlot, M. Miller, A. Simmons, and J.-N. Thepaut, 2003: A major new cycle of the IFS: Cycle 25R4. ECMWF Newsletter 97, ECMWF, Shinfield Park, Reading, Berkshire RG2 9AX, UK.
- Barkmeijer, J., R. Buizza, and T. Palmer, 1999: 3D-Var Hessian singular vectors and their potential use in the ECMWF Ensemble Prediction System. *Quart. J. Roy. Meteor. Soc.*, **125**, 2333–2351.
- Buizza, R. and A. Hollingsworth, 2002: Storm prediction over Europe using the ECMWF Ensemble Prediction System. *Meteorol. Appl.*, **9**, 289–305.
- Buizza, R., M. Miller, and T. Palmer, 1999: Stochastic representation of model uncertainties in the ECWMF Ensemble Prediction System. *Quart. J. Roy. Meteor. Soc.*, **125**, 2887–2908.
- Buizza, R. and T. Palmer, 1995: The singular-vector structure of the atmospheric global circulation. *J. Atmos. Sci.*, **52**, 1434–1456.
- Burt, S. D. and D. A. Mansfield, 1988: The great storm. *Weather*, **43**, 90–110.
- Charney, J., 1947: The dynamics of long waves in a baroclinic westerly current. *J. Meteor.*, **4**, 135–165.

- Courtier, P., E. Andersson, W. Heckley, J. Pailleux, D. Vasiljevic, M. Hamrud, A. Hollingsworth, F. Rabier, and M. Fisher, 1998: The ECMWF implementation of three-dimensional variational assimilation (3D-Var). I: Formulation. *Quart. J. Roy. Meteor. Soc.*, **124**, 1783–1807.
- Ferranti, L., E. Klinker, A. Hollingsworth, and B. J. Hoskins, 2002: Diagnosis of systematic forecast errors dependent on flow pattern. *Quart. J. Roy. Meteor. Soc.*, **128**, 1623–1640.
- Hay, R. F. M. and J. Laing, 1954: The storm of 31st January–1st February 1953. *Mar. Obs.*, **24**, 87–91.
- Hoskins, B. J. and P. Berrisford, 1988: Potential vorticity perspective. *Weather*, **43**, 122–129.
- Houtekamer, P. L., L. Lefaivre, J. Derome, H. Ritchie, and H. L. Mitchell, 1996: A system simulation approach to ensemble prediction. *Mon. Wea. Rev.*, **124**, 1225–1242.
- Jarraud, M., J. Goas, and C. Deyts, 1989: Prediction of an exceptional storm over France and Southern England (15–16 October 1987). *Weather and Forecasting*, **4**, 517–536.
- Lamb, H., 1991: *Historic Storms of the North Sea, British Isles and Northwest Europe*. Cambridge University Press.
- Lorenz, E. N., 1963: Deterministic non periodic flow. *J. Atmos. Sci.*, **20**, 130–141.
- Mahfouf, J.-F. and F. Rabier, 2000: The ECMWF operational implementation of four-dimensional variational assimilation. I: Experimental results with improved physics. *Quart. J. Roy. Meteor. Soc.*, **126**, 1171–1190.
- Molteni, F., R. Buizza, T. Palmer, and T. Petroliagis, 1996: The ECMWF ensemble prediction system: Methodology and validation. *Quart. J. Roy. Meteor. Soc.*, **122**, 73–119.
- Morris, R. M. and A. J. Gadd, 1988: Forecasting the Great storm. *Weather*, **43**, 70–89.
- Nebeker, F., 1995: *Calculating the weather*. Academic Press.
- Palmer, T. N., 1988: Medium and extended range predictability and stability of the Pacific/North American mode. *Quart. J. Roy. Meteor. Soc.*, **114**, 691–713.
- Palmer, T. N., 1993: Extended-range atmospheric prediction and the Lorenz model. *Bull. Amer. Meteor. Soc.*, **74**, 49–65.
- Palmer, T. N., 2000: Predicting uncertainty in forecasts of weather and climate. *Rep. Prog. Phys.*, **63**, 71–116.
- Palmer, T. N., F. Molteni, R. Mureau, P. Buizza, R. Chapelet, and J. Tribbia, 1993: Ensemble prediction. In: *ECMWF Seminar Proceeding on “Validation of models over Europe: Vol. I”*. ECMWF, Shinfield Park, Reading RG2 9AX, UK.
- Rabier, F., H. Järvinen, E. Klinker, J.-F. Mahfouf, and A. Simmons, 2000: The ECMWF operational implementation of four-dimensional variational assimilation. I: Experimental results with simplified physics. *Quart. J. Roy. Meteor. Soc.*, **126**, 1143–1170.
- Rabier, F., E. Klinker, P. Courtier, and A. Hollingsworth, 1996: Sensitivity of forecast errors to initial conditions. *Quart. J. Roy. Meteor. Soc.*, **122**, 121–150.
- Richardson, D. S., 2000: Skill and relative economic value of the ECMWF Ensemble Prediction System. *Quart. J. Roy. Meteor. Soc.*, **126**, 649–668.
- Richardson, L. F., 1922: *Weather Prediction by Numerical Process*. Cambridge University Press.



- Scherhag, R., 1962: Das Hamburger Katastrophentief vom 16./17. und sein Vorläufer vom 11. Februar 1962. In: *Berliner Wetterkarte*, pp. 1–10. Institut für Meteorologie und Geophysik der Freien Universität Berlin. 14/62 SO 7/62.
- Simmons, A. and A. Hollingsworth, 2001: Some aspects of the improvement of skill of numerical weather prediction. Technical Report 342, ECMWF, Shinfield Park, Reading, Berkshire RG2 9AX, UK.
- Toth, Z. and E. Kalnay, 1993: Ensemble forecasting at NMC: The generation of perturbations. *Bull. Amer. Meteor. Soc.*, **74**, 2317–2330.
- Uppala, S., 2002: ECMWF ReAnalysis 1957–2001. In: *3. Workshop on Re-analysis*. ECMWF, Shinfield Park, Reading RG2 9AX, UK.
- van Ufford, H. A. Q., 1953: The disastrous storm surge of 1 February 1953. *Weather*, **8**, 116–120.